NEARSHORE MIXING AND DISPERSION

Ib A. Svendsen and Uday Putrevu

Research Report No. CACR-92-07

September, 1992

CENTER FOR APPLIED COASTAL RESEARCH

Department of Civil Engineering
University of Delaware
Newark, Delaware 19716

NEARSHORE MIXING AND DISPERSION

Ib A. Svendsen & Uday Putrevu
Center for Applied Coastal Research
Department of Civil Engineering
University of Delaware
Newark, Delaware 19711

Abstract

Longshore currents on a long straight coast have in the past been analyzed assuming that the lateral mixing could be attributed to turbulent processes. It is found, however, that the mixing that can be justified by assuming an eddy viscosity $\nu_t = \ell\sqrt{k}$ where ℓ is the turbulent length scale, k the turbulent kinetic energy, combined with reasonable estimates for ℓ and k is at least an order of magnitude smaller than required to explain the measured cross-shore variations of longshore currents.

Based on a perturbation solution for the three-dimensional equations of motion averaged over a wave period, it is shown that the nonlinear interaction terms between cross- and longshore currents represents a dispersive mechanism that has an effect similar to the required mixing. The mechanism is a generalization of the one-dimensional dispersion effect in a pipe discovered by Taylor (1954) and the three-dimensional dispersion in ocean currents on the continental shelf found by Fischer (1978).

Numerical results are given for the dispersion effect, for the ensuing cross-shore variation of the longshore current and for the vertical profiles of the cross- and longshore currents inside as well as outside the surf zone. It is found that the dispersion affect is at least an order of magnitude larger than the turbulent mixing and that the characteristics of the results are in agreement with the sparse experimental data material available.

1 INTRODUCTION

Lateral mixing on gently sloping beaches plays an important role in the distribution of nearshore currents. The possible mechanisms responsible for the mixing current distribution have been discussed in the literature even before the concept of radiation stress was introduced and shown to be the primary forcing for the nearshore circulation (Harris, et al. 1963). In particular, the longshore currents on a long straight coast have been analyzed

so extensively that one would expect to find little new to add to the topic. In the present paper, however, we analyze the effect of current dispersion caused by the nonlinear interaction between the wave generated cross- and longshore currents. This is an extension of the three dimensional current pattern found by Svendsen & Lorenz (1989) who neglected the non-linear current interactions. We find that this mechanism includes an effect that has an effect similar to the traditional turbulent mixing, but even inside the surf zone is an order of magnitude stronger than the mixing that can be justified on the basis of the information we have about turbulence in the nearshore region. Thus, it is suggested that the unrealistically strong mixing that normally is assumed in model predictions of longshore currents can in fact be attributed to the dispersive effect of the vertical structure of the currents.

It is well known that when waves approach the shore and break, they exert a net force on a water column due to the decrease in radiation stress (Longuet-Higgins & Stewart 1960, 64).

The cross-shore component of this force is, in average over the depth, balanced by a pressure gradient caused by a slope in the mean water surface which results from a substantial wave setup in the surf zone. Due to the unequal distribution over depth of the forces involved, this mechanism also creates a cross-shore circulation which is fed by the shoreward mass flux in the breaking waves. It also includes the strong, seaward oriented undertow current which is particularly strong near the bottom (Svendsen 1984).

In the longshore direction, the longshore component S_{xy} of the net radiation stress on the water column is in the average balanced by a bottom shear stress τ_{by} which is created by a longshore current. The equation describing this balance is simply

$$\frac{\partial S_{xy}}{\partial x} + \tau_{by} = 0 \tag{1.1}$$

where the x-axis is assumed in the shore normal direction. As indicated by Bowen (1969),

Thornton (1970) and Longuet-Higgins (1970), a lateral mixing process will create a third type of force on the water column in the form of shear stresses. If these shear stresses are assumed described by a gradient law of the type

$$\tau_{xy} = \rho \nu_{tx} \frac{\partial V}{\partial x} \tag{1.2}$$

where ν_{tx} is a turbulent eddy viscosity and $V(x)$ the longshore current, then the force balance for a water column reads

$$\rho \frac{\partial}{\partial x} \left(\nu_{tx} \frac{\partial V}{\partial x} \right) - \tau_{by} - \frac{\partial S_{xy}}{\partial x} = 0 \tag{1.3}$$

Here τ_{by} is a function of V too.

Longuet-Higgins (1970; L-H in the following) demonstrated with clarity that because of the singular nature of (1.3), the mixing term is crucial in creating predictions of $V(x)$ that have resemblance with measured current distributions across the surf zone.

L-H also suggested that ν_{tx} might be described by an expression of the form

$$\nu_{tx} = N \, x \sqrt{gh} \tag{1.4}$$

where N is an empirical constant, h the water depth, and x the distance from the shoreline. L-H used this assumption also outside the breaker line and found that his model predicted the cross-shore variation of $V(x)$ quite well.

If we describe the bottom shear stress τ_{by} by a simple interaction between waves and longshore currents, which is linear in $V(x)$, the only parameter of the problem is $P = 2\pi \, h_x \, N / \gamma \, f_w$. Here f is the bottom friction coefficient and γ is the wave height to water depth ratio in the surf zone. Values of $P = 0.01$–0.4 (were found by L-H) to give realistic results, corresponding to $N \sim 0.01$ on, say, a slope of $1/35$.

The expression (1.4) has been widely used in the literature both for simple longshore currents and for more complex numerical circulation models. Often ν_{tx} outside the surf zone

is limited to its value at the breaker line.

The hydrodynamical mechanisms responsible for creating the lateral mixing have also been discussed. Thus, Inman et al. (1971) identified the surf zone generated turbulence and nearshore circulation cells associated with rip-currents as two possible sources of mixing. These ideas were further discussed, still in a rather qualitative manner, by Bowen & Inman (1974) who also emphasized the significance of the much lower level of turbulence outside the breaker zone in comparison to inside, and identified the nonlinear mass flux caused by the wave motion as a possible source of mixing. As will be seen in the following, the shore normal component, Q_{wx}, of the wave mass flux does indeed play a prominent role in the mixing though the mechanisms are far more complicated than have hitherto been suggested.

Also, the oscillatory particle motion itself has been suggested by some authors as a contributing source of mixing. Simple considerations will confirm, however, that there cannot be any net effect from a purely oscillatory wave motion. Neither should it be expected that the mixing can be made proportional to the wave motion by assuming that the turbulence level inside the surf zone is proportional to the strength of the wave motion itself.

The turbulent mixing coefficient ν_{tx} can be described by

$$\nu_{tx} = \ell\sqrt{k} \tag{1.5}$$

where k is the turbulent kinetic energy and ℓ is a characteristic length scale for the turbulence. Hence, estimates of the actual magnitude of the turbulence in- and outside of the surf zone are important steps towards quantifying the mixing. Battjes (1975) linked the turbulence energy to the energy dissipation D in the wave breaking which leads to $k \propto D^{\frac{1}{3}}$. In the assessment of the variation of the length scale however, Battjes follows the Longuet-Higgins model which assumes $\ell \propto x$, the distance from the shoreline, which leads to $\nu_{tx} \propto h_x^{\frac{4}{3}}$. Alternatively, Svendsen et al. (1987) suggest that $\ell \propto h$, the local water depth, which leads

to $\nu_{tx} \propto h_x^{\frac{1}{3}}$. Svendsen (1987) also finds that

$$\sqrt{k} = O(0.05)\sqrt{gh} \tag{1.6}$$

(although there is some variation with breaker type). Thus

$$\nu_{tz} \sim C_z \, h\sqrt{gh} \tag{1.7}$$

Comparing measurements for undertow with model predictions leads to the assessment for a 1:35 slope (Svendsen et al., 1987), C_z was found to be 0.01–0.02 corresponding to $\ell \sim 0.3h$ which seems reasonable. This estimate was later modified by Hansen & Svendsen (1987) to $C_z \sim$ 0.007–0.01. Outside the surf zone, C_z is be expected to be even smaller though no results are available.

If we assume that the characteristic length scale ℓ in the horizontal and vertical directions are similar, we have $\nu_{tx} \sim \nu_{tz}$ and (1.7) also becomes an estimate of ν_{tx}. Substituted into (1.4) and assuming $x = h/h_x$ (plane beach), however, we get (for $h_x = 1:35$) that $N \approx 3-4 \cdot 10^{-4}$. This is several orders of magnitude smaller than the $N \sim (1-2)10^{-2}$ found by Longuet-Higgins and many others to fit measurements.

Fig. 1 shows calculations of the longshore current distribution predicted by the L-H model for the two values of N mentioned above. The figure clearly illustrates the need for ν_{tx} values larger than given by (1.7) with $C_z = 0.01$ even though the use of (1.7) outside the surf zone is supposed to overestimate ν_{tx} there.

In the present paper, we first briefly outline the difference in the depth integrated equations required to incorporate depth varying currents and present the equations for the depth variation of the currents as well. Since we consider only time averaged equations, the wave motion is assumed known and the effects of the wave motion are represented by quantities such as mass flux, $Q_{w\alpha}$, and radiation stress, $S_{\alpha\beta}$, (α, β being horizontal tensor indices,

Phillips (1977)). The latter also has a local values $s_{\alpha\beta}$ at each point of a vertical over depth.

For simplicity, we concentrate in section 4 on the conditions on a long straight coast (no longshore variations) and establish a perturbation solution which is based on a set of parameters being small.

The first small parameter, ϵ, is associated with the assumption of a slowly varying water depth as is usually the case on littoral beaches.

The second small parameter is $\delta = \nu_{tx}/(h\sqrt{gh})$. According to (1.7), δ is small and we assume that $\delta = 0(\epsilon)$.

Associated with δ is a third small parameter, the existence of which is based on the observation that the turbulence generated by the wave breaking is much stronger and of larger scale than the turbulence created near the bottom. This assumption is closely linked to the idea that a (mainly oscillatory) boundary layer exists near the bottom in which waves and currents interact. The nature of such a boundary layer under a combination of non- breaking waves and currents have been studied by a number of authors (see e.g., Grant & Madsen (1979), Christofferson & Jonsson (1985), Trowbridge & Madsen (1984)). Also, experimental investigations have been reported (Brevik (1980), Brevik & Aas (1980), Kemp & Simmons (1983)). Little, however, is known about the situation under breaking waves, and we can only speculate what the near bottom conditions are. The hypothesis of an oscillatory bottom boundary layer with low intensity turbulence dominated by the near bottom turbulence production is supported by the fact that the cross-shore undertow velocities are large even very close to the bottom (Svendsen et al., 1987). Detailed measurements in particularly very close to the bottom (Okayasu et al. 1986, 1988) have shown that, although the velocity profiles are smooth, there are large vertical velocity gradients very near to the bottom.

A possible explanation for this could be that there is a gradual transition between the

bottom and the breaker generated turbulence in the direction away from the bottom. An alternative explanation is that the breaker generated turbulence only intermittently penetrates to the bottom and then as large scale vortices which temporarily may even momentarily wash away the entire small scale bottom boundary layer by simple convection. Such a pattern with a time scale of maybe 1/10 of a wave period would show up in the wave averaged data only as a reduced turbulence intensity.

In the absence of actual data and to reduce the complexity of the analysis without significantly changing the nature of the problem, we assume here that there is a low turbulence boundary layer so that the vertical current profiles have a finite "slip" velocity $V_{b\alpha}$ near the bottom. $V_{b\alpha}$ essentially represents the current velocity outside the bottom boundary layer and the bottom shear stress is related to $V_{b\alpha}$ and the wave bottom velocities u_{wb} through a dimensionless friction factor f. The third small parameter λ then represents the ratio $f\ h\sqrt{gh}/\nu_{tx}$. It will be assumed that $\lambda = O(\delta)$. With $\delta = O(\epsilon)$ this then implies that $f = O(\epsilon^2)$.

A perturbation expansion of the variables is then established in section 4 which leads to equations for the bottom velocity V_b in the longshore current. It is found that the lowest order solution V_b represents a simple local balance between rate of change of radiation stress and bottom friction with no mixing similar to eq. (1.1). Though mixing is formally included in the second order approximation for V_b, a meaningful solution for the cross-shore variation of the longshore velocity $V_b(x)$ is obtained only by combining terms of the first and second order. Hence, in this respect the proper equation for $V_b(x)$ resembles the KdV equation for weakly nonlinear, dispersive long waves which also includes terms of two different orders of magnitude.

The appropriate equation thus obtained for $V_b(x)$ includes both the turbulent mixing

represented by the eddy viscosity ν_{tx} and a contribution from the nonlinear interaction terms.

In the nearshore region studied here, both current-current and current-wave interaction contributes to this dispersion, and additional terms in the equations represent other effects of nonlinear interaction.

In section 5, analytical and numerical results are given for the simplified case where both ν_{tz} and the driving radiation stresses, $s_{\alpha\beta}$ are uniform over depth and the results for the cross-shore variation of the longshore current are discussed in section 6.

It appears that the dispersion effect found in the present paper is analogous to the longitudinal dispersion in a pipe caused by the lateral variation of the mean velocity (Taylor 1954) and generalized by Fisher (1978) for the three dimensional current patterns on a continental shelf. It is interesting to note that reasonable estimates for the turbulent mixing, yield dispersion determined from the vertical profile equations which are an order of magnitude stronger than the turbulent mixing even inside the surf zone. Nevertheless, since the turbulent mixing is largely responsible for shaping the vertical current velocity profiles, the turbulence actually controls the total depth integrated dispersion effect.

2 DISCUSSION OF FLOW PATTERN AND ADDITIONAL ASSUMPTIONS

The flow problem considered involves a combination of cross-shore and longshore currents generated by the obliquely incident waves. Figs. 2 and 3 show the situation schematically. The angle of incidence for the waves is α_w. The waves in general, and the breaking waves in particular, create a mass flux, which for (the usually) small α_w is primarily in the cross-shore direction. On a long straight coast, there can be no net cross-shore flow so that all the

shoreward oriented mass flux in the waves must return seaward through the undertow. (On an arbitrary topography, large scale current patterns may, of course, create any combination locally of cross- and longshore net flux.)

The radiation stress and setup pressure gradients play important roles in driving these flows and the vertical shear of the currents create shear stresses which are essential to the force balance.

The classical near-shore circulation theories (see e.g., Philips, 1977) implicitly assume depth uniform currents V_α which are isolated from the total water particle velocity u_α by averaging over a wave period and assuming that the wave part $u_{w\alpha}$ of the fluid velocity has a zero mean value. Though this process only makes sense below wave trough level, it is customary for depth uniform currents to assume the current velocity above trough level equals that below.

In the case considered here of non uniform currents, we make the analogous assumption that the mathematical expression for the current profile determined below wave trough level applies all the way to the instantaneous water surface. Since this is not a trivial assumption, a parameter α_e is introduced, the variation of which will gage the effects of deviations from the assumption. It is worth to emphasize that resolution of this question would follow from a solution in the time domain of breaking waves on arbitrary shear currents.

This aspect of the problem implies, however, that the level, ζ_t, of the wave trough (Fig. 3) plays a significant role in the mathematical expressions developed.

3 BASIC EQUATIONS

The equations describing nearshore circulation are depth integrated, time averaged equations for conservation of continuity and momentum. Since the flow is highly turbulent, the starting

point for the derivation is the Reynolds equations which can be written ($i = 1,2,3$)

$$\frac{\partial u_i}{\partial x_i} = 0 \tag{3.1}$$

and

$$\frac{\partial u_i}{\partial t} + \frac{\partial u_i u_j}{\partial x_j} = -\frac{1}{\rho}\frac{\partial p}{\partial x_i} + g_i + \frac{1}{\rho}\frac{\partial \tau_{ji}}{\partial x_j} \tag{3.2}$$

where u_i, p are the turbulent (or Reynolds) averaged velocities and pressure, respectively. τ_{ji} is the sum of viscous and turbulent stresses, and in the following the viscous part of τ_{ji} will be disregarded.

With both waves and currents present, the total velocities u_i can be divided into a current part $V_i = U,\ V,\ W$ (where the vertical component W will be much smaller than U, V) and a wave part $u_{wi} = u_w,\ v_w,\ w$, so that

$$u_i = V_i + u_{wi} \tag{3.3}$$

Using $\overline{\ }$ for average over a wave period, we define u_{wi} so that below wave trough level $\overline{u_{wi}}$ vanishes, i.e.,

$$\overline{u_{wi}} = 0 \qquad \text{below wave trough} \tag{3.4}$$

This corresponds to Phillips (1977) and differs from Mei (1983). Also following Phillips, we use indices $(\alpha,\ \beta) = (1,2)$ to indicate horizontal coordinate and velocity components and then denote the vertical coordinate by z (see Fig. 3). The boundary condition satisfied at the bottom is

$$w = -u_\alpha \frac{\partial h_0}{\partial x_\alpha} \quad \text{at} \quad z = -h_0(x_\alpha) \tag{3.5}$$

where h_0 is the undisturbed water depth. At the free surface we have

$$\left.\begin{aligned} \tfrac{\partial \zeta}{\partial t} - w - u_\alpha \tfrac{\partial \zeta}{\partial x_\alpha} &= 0 \\ p &= 0 \end{aligned}\right\} z = \zeta(x_\alpha, t) \tag{3.6}$$

The traditional depth integration of the equations assume that the current V_i is uniform over depth (see e.g., Phillips (1977) or Mei (1983)). It is, however, essential for the effect we are studying here to avoid that assumption, which leads to depth integrated equations different from those found in the literature. A brief outline of the derivation for the momentum equation is given following steps analogous to those used by e.g., Phillips (1977) for depth uniform currents.

We introduce the definition of horizontal discharge

$$Q_\alpha = \overline{\int_{-h_0}^{\zeta} u_\alpha dz} = \overline{\int_{-h_0}^{\zeta} V_\alpha dz} + Q_{w\alpha} \tag{3.7}$$

where

$$Q_{w\alpha} = \overline{\int_{\zeta_t}^{\zeta} u_{w\alpha} dz} \tag{3.8}$$

is the mass flux due to the wave part of the motion.

The first step is the integration over depth of the two horizontal components of (3.1), followed by the use of the Leibnitz rule to move $\partial/\partial t$ and $\partial/\partial x_\alpha$ outside the integrals and using the bottom and free surface boundary conditions (3.5) and (3.6) to reduce the boundary terms. Finally, the equations are time-averaged.

The result of these operations can be written as

$$\frac{\partial Q_\beta}{\partial t} + \frac{\partial}{\partial x_\alpha}\overline{\int_{-h_0}^{\zeta} V_\alpha V_\beta dz} + \frac{\partial}{\partial x_\alpha}\overline{\int_{\zeta_t}^{\zeta} (u_{w\alpha}V_\beta + u_{w\beta}V_\alpha)dz} =$$

$$-\frac{\overline{p_D(-h_0)}}{\rho}\frac{\partial h_0}{\partial x_\beta} - gh\frac{\partial \bar{\zeta}}{\partial x_\beta} - \frac{\partial}{\partial x_\alpha}\left(\frac{S_{\alpha\beta} + S'_{\alpha\beta}}{\rho}\right) - \frac{\overline{\tau_{b,\beta}}}{\rho} \tag{3.9}$$

where p_D is the dynamic pressure defined as

$$p_D = p - \rho g(\zeta - z) \tag{3.10}$$

$S_{\alpha\beta}$ is the radiation stress due to the waves and is defined by

$$S_{\alpha\beta} = \overline{\int_{-h_0}^{\zeta} (\rho u_{w\alpha} u_{w\beta} - p\delta_{\alpha\beta}) dz} - \delta_{\alpha\beta} \frac{1}{2} \rho g h^2 \tag{3.11}$$

$S'_{\alpha\beta}$ is the radiation stress due to turbulent fluctuations defined by

$$S'_{\alpha\beta} = -\overline{\int_{-h_0}^{\zeta} \tau_{\alpha\beta} dz} \tag{3.12}$$

Finally, $\overline{\tau_{b,\alpha}}$ is mean the bottom shear stress. Normal and tangential stresses at the free surface have been neglected.

The pressure $p_D(-h_0)$ can be eliminated from this equation by integration over depth of the vertical component of (3.2). Under realistic assumptions which include gently sloping topography and reasonably slowly varying waves, we find

$$\overline{p_D(-h_0)} = 0 \tag{3.13}$$

which means in average over a wave period the weight of each water column is carried entirely by the pressure on the bottom under the column.

Introducing this result into (3.9) then yields

$$\frac{\partial Q_\alpha}{\partial t} + \frac{\partial}{\partial x_\beta} \left[\overline{\int_{-h_0}^{\zeta} V_\alpha V_\beta dz} + \overline{\int_{\zeta_t}^{\zeta} (u_{w\beta} V_\alpha) dz} \right]$$

$$+ gh \frac{\partial \bar{\zeta}}{\partial x_\alpha} + \frac{\partial}{\partial x_\beta} \left(\frac{S_{\alpha\beta} + S'_{\alpha\beta}}{\rho} \right) + \frac{\tau_{b,\alpha}}{\rho} = 0 \tag{3.14}$$

It may be noticed that this equation differs from the usual form for depth uniform currents in that second and third terms cannot be reduced further. For depth uniform currents, we would get

$$\frac{\partial}{\partial x_\beta} \overline{\int_{-h_0}^{\zeta} V_\alpha V_\beta dz} + \overline{\int_{-h_0}^{\zeta} (u_{w\alpha} V_\beta + u_{w\beta} V_\alpha) dz} =$$

$$\frac{\partial}{\partial x_\beta}\left[\frac{Q_\alpha Q_\beta}{h} - \frac{Q_{w\alpha} Q_{w\beta}}{h}\right] \tag{3.15}$$

see e.g., Phillips (1977). Phillips includes the last term in (3.15) in his definition of $S_{\alpha\beta}$ whereas Mei (1983) neglects it. In Stokes waves, this term is $O(H^4)$ and hence is usually considered negligible. In the present context, however, and particularly for the breaking waves in the surf zone, this turns out not to be a valid assumption.

Equations for the current profiles.

In order to evaluate the integrals in (3.14) of currents, we also need to determine the current variation over depth. This is done by solving the Reynolds equations between the bottom and wave trough level using suitable simplifying assumptions and boundary conditions as discussed in the following.

The Reynolds equations for the general situation of breaking waves with currents were presented by Svendsen & Lorenz (1989). They are, using the same notation as above,

$$\frac{\partial V_\beta}{\partial t} + \frac{\partial V_\alpha V_\beta}{\partial x_\alpha} + \frac{\partial W V_\beta}{\partial z} + \frac{\partial \overline{u_{w\alpha} u_{w\beta}}}{\partial x_\alpha} - \frac{\partial \overline{w_w^2}}{\partial x_\beta} + \frac{\partial \overline{u_{w\beta} w_w}}{\partial z} =$$

$$-g\frac{\partial \bar{\zeta}}{\partial x_\beta} - \frac{\partial \overbrace{\overline{u'_\alpha u'_\beta}}}{\partial x_\alpha} + \frac{\partial \overbrace{\overline{w'^2}}}{\partial x_\beta} - \frac{\partial \overbrace{\overline{u'_\beta w'}}}{\partial z} \tag{3.16}$$

In these equations, the $\partial \overline{u_{w\beta} w_w}/\partial z$ terms represent the horizontal mean shear stresses created by the wave motion. In any permanent form periodic wave motion, these terms are zero. On a beach, however, two mechanisms contribute to these terms. One is the disturbance of the wave motion caused by the sloping bottom. The second is the deformation of the waves, as the wave height decreases, required to transport energy vertically to the regions near the surface or bottom where energy is being dissipated. This second mechanism was discussed by Deigaard & Fredsoe (1989).

The first can be estimated for long waves with depth uniform horizontal velocities. Recalling that $\partial u_{w\alpha}/\partial z = 0$ and using the continuity equation yields

$$\frac{\partial u_{w\beta} w_w}{\partial z} = u_{w\beta} \frac{\partial w_w}{\partial z} = -u_{w\beta} \frac{\partial u_{w\alpha}}{\partial x_\alpha} \tag{3.17}$$

Combined with the $\overline{\partial u_{w\alpha} u_{w\beta}}/\partial x_\alpha$ term, this yields

$$\frac{\partial \overline{u_{w\alpha} u_{w\beta}}}{\partial x_\alpha} + \frac{\partial \overline{u_{w\beta} w_w}}{\partial z} = \overline{u_{w\alpha} \frac{\partial u_{w\beta}}{\partial x_\alpha}} \tag{3.18}$$

Thus, in the case of a plane wave, this is equivalent to reducing the $\partial \overline{u_{w\alpha}^2}/\partial x_\alpha$ term by a factor of two.

Inside the surf zone, these effects are relatively small because the driving forces below trough level are dominated by the $\partial \bar{\zeta}/\partial x_\beta$ (Svendsen et al., 1987). Outside the surf zone, however, the contributions from the velocity terms become important and in that region we use the approximation given above (see section 6).

For the purely 2D cross-shore flow of shore normal waves on a long straight coast, equations (3.16) have been solved by different authors using different boundary conditions (Svendsen, 1984; Dally & Dean, 1984; Stive & Wind, 1986; Svendsen et al., 1987) and different assumptions for the eddy viscosity used in the turbulent closure (Okayasu et al., 1988; Deigaard et al., 1991).

The 3D combination of both cross-shore and longshore currents was analyzed by a perturbation method by Svendsen & Lorenz (1989) who, however, neglected the UV interaction term. Svendsen & Putrevu (1990) generalized the formulation and outlined the assumptions for the interaction between the vertical profiles and 2D horizontal models which will be formalized in the following.

To determine the current profiles from (3.16), we first recall that all the terms with index w represent (known) inhomogeneities in (3.16). The term $\partial \bar{\zeta}/\partial x_\beta$ represents the slope on

the mean water level.

We assume that the turbulent shear stresses can be modelled by horizontal and vertical eddy viscosities ν_{tx} and ν_{tz} so that

$$-\overbrace{\overbrace{u'_\alpha u'_\beta}} = \nu_{tx_\alpha}\left(\frac{\partial V_\alpha}{\partial x_\beta}+\frac{\partial V_\beta}{\partial x_\alpha}\right) \tag{3.19a}$$

$$-\overbrace{\overbrace{u'_\beta w'}} = \nu_{tz}\frac{\partial V_\beta}{\partial z} \tag{3.19b}$$

and for the sake of later discussion, we assume ν_{tx} and ν_{tz} can be different.

Substituting into (3.16) and also applying that by continuity

$$\frac{\partial V_\alpha}{\partial x_\alpha}+\frac{\partial W}{\partial z}=0 \tag{3.20}$$

(3.16) takes the form

$$\frac{\partial V_\beta}{\partial x_\alpha}-\frac{\partial}{\partial z}\left(\nu_{tz}\frac{\partial V_\beta}{\partial z}\right)-\frac{\partial}{\partial x_\alpha}\left(\nu_{tx_\alpha}\left(\frac{\partial V_\alpha}{\partial x_\beta}+\frac{\partial V_\beta}{\partial x_\alpha}\right)\right)=$$

$$-\frac{\partial}{\partial x_\alpha}\left(\overline{u_{w\alpha}u_{w\beta}}+g\bar{\zeta}\right)-\frac{\partial\overline{w_w^2}}{\partial x_\beta}+\frac{\partial\overline{u_{w\beta}w_w}}{\partial z}$$

$$-V_\alpha\frac{\partial V_\beta}{\partial x_\alpha}-W\frac{\partial V_\beta}{\partial z} \tag{3.21}$$

To simplify the equations and make possible a comparison of the results with experimental data, the following derivations are limited to the steady state case of obliquely incident waves generating a longshore current and a cross-sore circulation on a long, straight coast.

4 SOLUTION OF THE EQUATIONS ON A LONG STRAIGHT COAST

The assumption of a gently sloping bottom is introduced into the analysis by assuming that the characteristic vertical length scale (e.g., the water depth h_b at breaking) is much smaller than the characteristic horizontal length scale ℓ_s (say, the width of the surf zone). We define the scaling parameter ϵ accordingly as

$$\epsilon = \frac{h_b}{\ell_s} \ll 1 \tag{4.1}$$

Dimensionless variables marked by $'$ are introduced based on ℓ_s, h_b and $c_0 = (gh_b)^{\frac{1}{2}}$

$$x' = \frac{x}{\ell_s} \; ; \; y' = \frac{y}{\ell_s} \; ; \; z' = \frac{z}{h_b} \; ; \; h' = \frac{h}{h_b}$$

$$u'_w = \frac{u_w}{c_0} \; ; \; v'_w = \frac{v_w}{c_0} \; ; \; U' = \frac{U}{c_0} \; ; \; V' = \frac{V}{c_0} \tag{4.2}$$

$$\nu'_t = \frac{\nu_t}{h_b c_0} \; ; \; \tau'_b = \frac{\tau_b}{\rho c_0^2} \; ; \; S'_{\alpha\beta} = \frac{S_{\alpha\beta}}{\rho c_0^2 h}$$

We let the x-axis be normal to and directed towards the shore, y parallel with the shoreline so that the assumed uniformity in the shore parallel direction implies $\partial/\partial y = 0$ everywhere. The steady state version of (3.14) in the non-dimensional variables introduced above then becomes (x and y components respectively):

$$\epsilon \frac{\partial S'_{xx}}{\partial x'} = -\epsilon \, h' \frac{\partial \overline{\zeta'}}{\partial x'} - \tau'_{bx} \tag{4.3}$$

$$\epsilon^2 \frac{\partial}{\partial x'} \left(\int_{-h_0}^{\zeta} \nu'_{tx} \frac{\partial V'}{\partial x'} dz \right) - \tau'_{by} - \epsilon \frac{\partial}{\partial x'} \left[\overline{\int_{-h_0}^{\zeta} U'V' dz'} + \overline{\int_{\zeta t'}^{\zeta} u'_w V' + v'_w U' dz'} \right] = \epsilon \frac{\partial S'_{xy}}{\partial x'} \tag{4.4}$$

in which we have also neglected the turbulent normal stresses.

Similarly (3.20) yields for $U'(x',z')$ and $V'(x',z')$ (again neglecting turbulent normal stresses):

$$\frac{\partial}{\partial z'}\left(\nu'_{tz}\frac{\partial U'}{\partial z'}\right) = \epsilon\left[\frac{\partial}{\partial x'}\left(\overline{\zeta'} + \overline{u'^2_w}\right) + U'\frac{\partial U'}{\partial x'} + \frac{\partial}{\partial z}\overline{u_w w_w} + W'\frac{\partial U'}{\partial z'}\right] \tag{4.5}$$

and

$$\frac{\partial}{\partial z'}\left(\nu'_{tz}\frac{\partial V'}{\partial z'}\right) + \epsilon^2\frac{\partial}{\partial x'}\left(\nu'_{tx}\frac{\partial V'}{\partial x'}\right) = \epsilon\left[\frac{\partial}{\partial x'}\overline{u'_w v'_w} + U'\frac{\partial V'}{\partial x'} + \frac{\partial}{\partial z}\overline{v_w w'} + W\frac{\partial V'}{\partial z'}\right] \tag{4.6}$$

Solution of (4.5) and (4.6) require two boundary conditions for each in the vertical direction in addition to conditions in the x-direction. One boundary condition for each of the two equations relate the wave averaged bottom shear stress $\tau_{b\beta}$ to the derivative of the current velocity at the bottom:

$$\left(\frac{\partial V_\beta}{\partial x}\right)_b = \frac{\tau_{b\beta}}{\rho\nu_{tz}} \tag{4.7}$$

Assuming, as discussed earlier, the existence of a (partly) oscillatory wave-current boundary layer at the bottom, suggests that $\tau_{b\beta}$ is related to $V_{b\beta}$ and the bottom wave velocity amplitude u_{wb}. A simple relationship of this form used by Longuet-Higgins for small angles of incidence and weak currents gave

$$\tau_{by} = \frac{1}{\pi}\rho\, f\, u_{wb}\, V_b \tag{4.8}$$

This expression is a special case of the more general description that assumes that the instantaneous shear stress $\tau_{b\beta}(t)$ has the form

$$\tau_{b\beta}(t) = \frac{1}{2}\rho\, f\, u_\beta(t)\mid u_\beta(t)\mid \tag{4.9}$$

where $u_\beta(t) = u_{w\beta} + V_\beta$ is the total instantaneous velocity of the bottom and f a (constant) friction factor. This model was studied for other special cases by Liu and Dalrymple (1978) and generalized by Svendsen & Putrevu (1990).

For the present purpose, it suffices to assume that an expression exists that links $\tau_{b\beta}$ to $V_{b\beta}$

$$\tau_{b\beta} = \tau(u_{wb},\, V_{b\beta}) \tag{4.10}$$

Combining (4.7) and (4.10) gives a mixed boundary condition at the bottom of the form

$$\left(\frac{\partial V_\beta}{\partial z}\right)_b - \frac{\tau(u_{wb},\, V_{b\beta})}{\rho(\nu_{tz})_b} = 0 \tag{4.11}$$

which in the simple case of (4.8) corresponds to

$$\left(\frac{\partial V_\beta}{\partial z}\right)_b - b\, V_{\beta b} = 0 \quad ; \quad b = \frac{1}{\pi}\,\frac{f u_{wb}}{(\nu_{tz})_b} \tag{4.12}$$

The second boundary condition for the vertical current variation differs in the x and y direction. In the shore normal x- direction, the condition of shore parallel uniformity implies that there can be no net cross shore flow. Hence, (3.7) yields:

$$U_m h = \overline{\int_{-h_0}^{\zeta} U dz} = -Q_{wx} \tag{4.13}$$

where U_m is the depth averaged value of $U(z)$, and the wave volume flux Q_{wx} is supposed to be known.

In the shore parallel direction, there is no such constraint and the second boundary condition in the y-direction for (4.6) consists of (4.4) which states that the total depth integrated momentum in the y-direction is a balance of the forces in (4.4) most of which depends on the U' and V' variation over the depth.

Perturbation Solution

A perturbation solution of these equations will also help reveal the relative importance of the many mechanisms at play. We introduce the following series expansions.

$$\begin{aligned} V' &= V'_0(x') + \epsilon V'_1(x', z') + \epsilon^2 V'_2(x', z') + \cdots \\ U' &= \epsilon U'_1(x', z') + \epsilon^2 U'_2(x', z') + \cdots \end{aligned} \tag{4.14}$$

Whereas, the vertical variation of V' is assumed $\epsilon V_0'$ with $V_0' = O(1)$, the vertical variation of U is expected to be of the same order as U.

For reasons of continuity, we have

$$W' = \epsilon^2 W_2'(x', z') + \epsilon^3 W_3'(x', z') + \cdots \tag{4.15}$$

We also expand the bottom velocities U_b' and V_b' and the bottom shear stress τ_{by}

$$\begin{aligned} V_b' &= V_0'(x') + \epsilon^2 V_{b1}(x') + \cdots \\ U_b' &= \epsilon U_{b1}'(x') + \epsilon^2 U_{b2}'(x') + \cdots \\ \tau_{by}' &= \epsilon^2 \tau_{y2}'(V_0) + \epsilon^4 \tau_{y4}' + \cdots \\ \tau_{bx}' &= \epsilon^3 \tau_{x3}'(U_{b1}') + \cdots \end{aligned} \tag{4.16}$$

The magnitudes assumed for the τ_b components and V_b will be justified below.

Finally, we assume that

$$\nu_{tx}', \ \nu_{tz}' = O(\delta) \tag{4.17}$$

where δ is an independent small parameter which is assumed $O(\epsilon)$. Using (4.8) to assess the magnitude of τ_{by}, we get

$$\tau_{by}' = \frac{1}{\pi} f \, u_{wb}' \, V_b' = O(f) \tag{4.18}$$

if we assume $u_{wb}' = O(1)$ as will be the case in breaking or near breaking waves. Measurements suggest that both the scale and intensity of turbulence in the bottom boundary layer is much smaller than in the region between bottom and surface where the turbulence mainly originates from the breaking process (for further discussion reference is made to Svendsen et al. (1987)). Thus, we let

$$\frac{f}{\nu_{tz}'} = O(\epsilon) \quad \text{or} \quad f = O(\epsilon^2) \tag{4.19}$$

and hence

$$\tau_{by}' = O(\epsilon^2) \tag{4.20}$$

Since $\tau_{by} = O\left(\partial S_{xy}/\partial x\right)$ this implies

$$\frac{\partial S'_{xy}}{\partial x'} = O\left(\frac{\tau'_{by}}{\epsilon}\right) = O(\epsilon) \tag{4.21}$$

This is possible, although $(u_w,\ v_w)$ are assumed $O(1)$, because the time averaging process of $u_w\ v_w$ that leads to S_{xy} reduces $u_w\ v_w$ by an order of magnitude relative to their maximum values. For similar reasons $Q_{w\alpha}$ defined by (3.8) is assumed $O(\epsilon)$.

We also find, however, that a consequence of assuming $U = O(\epsilon)$ is that

$$\tau'_{bx} = O(f\ u_{wb}\ U_b) = O(\epsilon^3) \tag{4.22}$$

Since $S'_{xx} = O(S'_{xy}) = O(\epsilon)$, (4.3) implies that $\partial\bar{\zeta}/\partial x = O(\epsilon)$. Comparison of this with (4.22) shows that τ_{bx} is a small term in (4.3) as would be expected.

We also notice that in consequence of (4.22), we have

$$\left(\frac{\partial U'}{\partial z'}\right)_b = \frac{\tau'_{bx}}{\nu'_{tz}} = O(\epsilon^2) = O(\epsilon U')$$
$$\left(\frac{\partial V'}{\partial z'}\right)_b = \frac{\tau'_{by}}{\nu'_{tz}} = O(\epsilon) = O(\epsilon V')$$

which means that both U' and V' have gradients near the bottom which are an order of magnitude smaller than U', V' themselves.

Substitution of the expansions and order estimates into (4.5) yield (now returning to dimensional variables)

$$\frac{\partial}{\partial z}\left(\nu_{tz}\frac{\partial U_1}{\partial x}\right) = \frac{\partial}{\partial x}\left(g\bar{\zeta} + \overline{u_w^2}\right) + \frac{\partial \overline{u_w w_w}}{\partial z} \tag{4.23}$$

and

$$\frac{\partial}{\partial z}\left(\nu_{tz}\frac{\partial U_2}{\partial z}\right) = U_1\frac{\partial U_1}{\partial x} \tag{4.24}$$

Thus the equation for U_1 is the same as has been used in the literature to analyze undertow and cross-shore circulation currents. To the second order (Eq. 4.24), a correction U_2 can be determined which accounts for the (nonlinear) modification of the current by itself.

In the longshore direction, we get for V:

$$\frac{\partial}{\partial z}\left(\nu_{tz}\frac{\partial V_1}{\partial z}\right) = \frac{\partial}{\partial x}\overline{u_w v_w} + \frac{\partial}{\partial z}\overline{v_w w_w} + U_1\frac{\partial V_0}{\partial x} \tag{4.25}$$

and

$$\frac{\partial}{\partial z}\left(\nu_{tx}\frac{\partial V_2}{\partial z}\right) = -\frac{\partial}{\partial x}\left(\nu_{tx}\frac{\partial V_0}{\partial x}\right) + U_1\frac{\partial V_1}{\partial x} + W\frac{\partial V_1}{\partial z} + U_2\frac{\partial V_0}{\partial x} \tag{4.26}$$

Here the essential new feature relative to Svendsen & Lorenz (1989) is the term $U_1\partial V_0/\partial x$ in (4.25) which shows that the current-current interaction plays an important role in the depth variation of the longshore current.

It is also noted that, in parallel with the result by Svendsen & Lorenz (1989), there is a third order approximation V_2 to the longshore current variation which is driven by the turbulent mixing induced by the V_0-term. In addition to the earlier solution, however, V_2 is also influenced by the UV contributions originating from the interaction between U_1, V_1 and U_2, V_0, and by a contribution from the weak vertical current component W in combination with $\partial V_1/\partial z$.

The most significant effects of the UV-interaction appear in the depth integrated momentum equation for the longshore current. To the lowest order, we simply get

$$\tau_{y2} - \frac{\partial S_{xy}}{\partial x} = O(\epsilon^3) \tag{4.27}$$

which corresponds to the triangular velocity profile found by Longuet-Higgins in the case of no mixing at all. That solution, however, is unacceptable as the fundamental solution for V_0. A realistic solution for V_0 requires that we include both ϵ^2 and ϵ^3 terms. Thus the equation for V_0 becomes

$$\frac{\partial}{\partial x}\left(\overline{\int_{-h_0}^{\zeta}\nu_{tx}dz\frac{\partial V_0}{\partial x}}\right) - \frac{\tau_{y2}(V_0)}{\rho} - \frac{\partial}{\partial x}\left[\overline{\int_{-h_0}^{\zeta}U_1V_1dx} + \overline{\int_{\zeta_t}^{\zeta}u_wV_1 + v_wU_1dz}\right] = \frac{1}{\rho}\frac{\partial S_{xy}}{\partial x} + O(\epsilon^4) \tag{4.28}$$

Here we have utilized that

$$\overline{\int_{-h_0}^{\zeta} U_1 V_0 dz} + \overline{\int_{\zeta_t}^{\zeta} u_w V_0 dz} = -Q_{wx} V_0 + Q_{wx} V_0 = 0 \tag{4.29}$$

by virtue of the definition of U_1.

It is interesting to notice the analogy of this result with Boussinesq wave theory which also requires terms of two orders of magnitude as, e.g., in the KdV equation to obtain meaningful results. As in the KdV-equation the two terms in (4.7), which individually are $O(\epsilon^2)$, together represent a contribution $O(\epsilon^3)$ which is also the magnitude of the other terms in (4.33).

For the next approximation of the depth integrated equation we get

$$\frac{\partial}{\partial x}\left(\int_{-h_0}^{\zeta} \nu_{tx} \frac{\partial V_1}{\partial x} dz\right) - \frac{\tau_{y4}(V_{b1})}{\rho} - \frac{\partial}{\partial x}\left[\overline{\int_{-h_0}^{\zeta} (U_1 V_2 + U_2 V_1)\, dz} + \overline{\int_{\zeta_t}^{\zeta} (u_w V_2 + v_w (U_m + U_1))\, dz}\right] = 0 \tag{4.30}$$

Here the first term and the integrals are all $O(\epsilon^4)$ which shows that τ_{y4} must be $O(\epsilon^4)$. Comparing with (4.8) and recalling (4.19), we see that this implies $V_{b1} = O(\epsilon^2)$ as already assumed in (4.16). The physical explanation for this is that the net forcing represented by the terms in (4.30) are quite small. This also justifies that we do not need to include a $\tau(V_{b1})$-term in (4.28).

Solution to the Equations

The equations (4.23) and (4.25) for U_1 and V_1, respectively, may be readily solved. Defining

$$\alpha_x = \frac{\partial}{\partial x}\left(g\bar{\zeta} + \overline{u_w^2}\right) + \frac{\partial \overline{u_w w_w}}{\partial z} \tag{4.31}$$

we get from (4.23)

$$U_1 = \int_0^{\xi} \frac{1}{\nu_{tz}} \int_0^{\xi} \alpha_x d\xi d\xi + \frac{\tau_{x3}}{\rho} \int_0^{\xi} \frac{d\xi}{\nu_{tz}} + U_{b1} \tag{4.32}$$

Here the sum of the last two integrals is zero which shows that V_{b1} does not contribute to these integrals. We introduce the definition

$$D_C = -\frac{1}{h}\overline{\int_{-h_0}^{\zeta} U_1 A \, dz} - \frac{1}{h}\overline{\int_{\zeta_t}^{\zeta} u_w \, A \, dz}$$

Introducing the definition (4.36) for A, we get

$$D_C = -\frac{1}{h}\overline{\int_{-h_0}^{\zeta} U_1 \int_0^{\xi} \frac{1}{\nu_{tz}} \int_0^{\xi} U_1 \, d\xi \, d\xi \, dz} - \frac{1}{h}\overline{\int_{\zeta_t}^{\zeta} u_w \int_0^{\xi} \frac{1}{\nu_{tz}} \int_0^{\xi} U_1 \, d\xi d\xi dz} \tag{4.39}$$

It is also convenient to define a coefficient α_e (expected to be close to unity) so that the second integral in (4.38) can be written

$$\overline{\int_{\zeta_t}^{\zeta} u_w(a_y(z) + b_y(z))dz} = \alpha_e(a_y(h) + b_y(h))Q_{wx} \tag{4.40}$$

Substituting these results and definitions into (4.28), that equation may then be written

$$\frac{\partial}{\partial x}\left(h(\nu_{tx} + D_C)\frac{\partial V_0}{\partial x}\right) - \frac{\tau_{b2}(V_0)}{\rho} - \frac{\partial}{\partial x}\overline{\int_{-h_0}^{\zeta} U_1(a_y + b_y)dz}$$
$$-\frac{\partial}{\partial x}\left[\alpha_e(a_y(h) + b_y(h))Q_{wx}\right] = \frac{1}{\rho}\frac{\partial S_{xy}}{\partial x} \tag{4.41}$$

Clearly, D_C here plays the same role as an additional mixing coefficient. Furthermore, the current-current interaction terms provide additional terms in the equation (the third and fourth terms) which essentially have the nature of driving terms. The mechanisms and effects will be discussed and illustrated in more detail in the following sections. First, it is convenient, however, to further identify the nature of D_C. We introduce the variables

$$n_{tz} = \frac{\nu_{tz}}{\overline{\nu_{tz}}} \quad ; \quad \overline{\nu_{tz}} = \frac{1}{h}\int_0^h \nu_{tz} d\xi \tag{4.42}$$

and also the local vertical dimensionless coordinate

$$\xi^* = \xi/h \tag{4.43}$$

We then get

$$A(h) = \frac{U_m h^2}{\overline{\nu_{tz}}} I_A$$

where

$$I_A = \overline{\int_0^{\zeta^*} \frac{1}{n_{tz}} \int_0^{\xi^*} \frac{U_1}{U_m} d\xi^* \, d\xi^*} \tag{4.44}$$

Similarly, we define

$$I_D = -\overline{\int_{-h_0}^{\zeta^*} \frac{U_1}{U_m} \int_0^{\xi^*} \frac{1}{n_{tz}} \int_0^{\xi^*} \frac{U_1}{U_m} \, d\xi^* \, d\xi^* \, dz^*} \tag{4.45}$$

by which D_C can be written

$$D_C = \frac{U_m^2 h^2}{\overline{\nu_{tz}}} (\alpha_e I_A - I_D) \tag{4.46}$$

where the coefficient α_e has been introduced by (4.40). As expected, $U_m = O(\epsilon)$ and $\overline{\nu_{tz}} = O(\epsilon)$ leads to $D_C = O(\epsilon) = O(\nu_{tz})$. In the examples below, we will find, however, that the numerical value of D_C is significantly larger than ν_{tx} if $\nu_{tx} = \nu_{tz}$ is assumed.

When we analyze the other interaction terms in (4.41), it is important to realize that b_y depends on the longshore bottom velocity V_b through τ_{y2} in (4.36). By virtue of (4.18), we have

$$\tau_{y2} = \frac{1}{\pi} \rho f \, u_{wb} \, V_0$$

Substituting into the two remaining interaction terms in (4.41), these terms can be written

$$\begin{aligned} M &= \overline{\int_{-h_0}^{\zeta} U_1 (a_y(z) + b_y(z)) dz} + \alpha_e (a_y(h) + b_y(h)) Q_{wx} \\ &= \overline{\int_{-h_0}^{\zeta} U_1 \int_0^{\xi} \frac{1}{\nu_{tz}} \int_0^{\xi} \alpha_y d\xi d\xi dz} + \overline{\int_{-h_0}^{\zeta} \frac{1}{\nu_{tz}} \int_0^{\xi} \alpha_y d\xi dz} Q_{wx} \\ &\quad + \frac{f u_{wb}}{\pi} \left[\overline{\int_{-h_0}^{\zeta} U_1 \int_0^{\xi} \frac{1}{\nu_{tz}} d\xi dz} + Q_{wx} \overline{\int_{-h_0}^{\zeta} \frac{dz}{\nu_{tz}}} \right] V_b \end{aligned} \tag{4.47}$$

Introducing again the dimensionless variables of (4.42) and (4.43) and in addition

$$\overline{\alpha_y} = \frac{1}{h} \overline{\int_{-h_0}^{\zeta} \alpha_y dz}$$

the solutions inside and outside the breaker point. The boundary and matching conditions for the solution of (4.52) is as follows:

$$V_b = 0 \quad \text{at} \quad \begin{cases} h = 0 \\ h/h_b \to \infty \end{cases} \tag{6.2}$$

$$V_b(x_b+) = V_b(x_b-) \tag{6.3}$$

$$\frac{\partial V}{\partial x}\Big)_{x_{b+}} = \frac{\partial V}{\partial x}\Big)_{x_{b-}} \tag{6.4}$$

Here x_b represents the breaker line position, and the last condition is equivalent of continuity in τ_{xy}, the horizontal shear stresses in the longshore direction along vertical shore parallel surfaces.

To simplify the discussions, a'_x is assumed constant in the surf zone. This is in accordance with the assumption of γ = const which yields $\partial\bar{\zeta}/\partial x$ constant (Bowen et al., 1968). As indicated in section 5, a characteristic value corresponds to $a'_x \sim 0.15$. Invoking (4.2) for nondimensionalizing (U, U_b) and (4.43) for ξ, we can then write (5.1) as

$$U' = a'_x\, \xi^{*2} + b'_x \xi^* + U'_b \tag{6.5}$$

which is evaluated inside the surf zone with the above mentioned $a'_x = 0.15$.

The longshore driving force represented by α_y is in the computations assumed to correspond to an angle of incidence for the waves of 11.4° at the breaker point which yields $v_w \sim 0.2\, u_w$ or $\overline{u_w v_w} \sim 0.2\, \overline{u_w^2}$. For linear theory with $u_w \sim c\eta/h$ and $\gamma = 0.7$ this gives

$$\frac{\partial}{\partial x}\overline{u_w w_w} \sim 0.2 \cdot g h_x \gamma^2 \overline{\eta^2}/H^2 \sim 0.012 g h_x$$

which is approximately $\alpha_x/10$.

we can write (4.47) as

$$\begin{aligned} M &= \frac{U_m h^2}{\overline{\nu_{tz}}}\left[\overline{\alpha_y} h\, I_{ca} + \frac{f u_{wb}}{\pi} I_{cb} V_0\right] \\ &= F_1 + F_2 V_0 \end{aligned} \tag{4.48}$$

where

$$I_{ca} = \overline{\int_{-h_0^*}^{\zeta^*}\left[\frac{U_1}{U_m}\int_0^{\xi^*}\frac{1}{n_{tz}}\int_0^{\xi^*}\frac{\alpha_y}{\overline{\alpha_y}}d\xi^* d\xi^* - \frac{1}{n_{tz}}\int_0^{\xi^*}\frac{\alpha_y}{\overline{\alpha_y}}d\xi^*\right]dz^*} \tag{4.49}$$

$$I_{cb} = \overline{\int_{-h_0^*}^{\zeta^*}\left[\frac{U_1}{U_m}\int_0^{\xi^1}\frac{dz^*}{\nu_{tz}} - \frac{1}{n_{tz}}\right]dz^*} \tag{4.50}$$

and

$$\begin{aligned} F_1 &= \frac{U_m h^3}{\overline{\nu_{tz}}}\overline{\alpha_y} I_{ca} \\ F_2 &= f\frac{U_m u_{wb} h^2}{\pi \overline{\nu_{tz}}} I_{cb} \end{aligned} \tag{4.51}$$

For purposes of generalizing to arbitrary topographies, it has been chosen to express the final results in terms of U_m rather than Q_{wx} (since it is only for the case of long straight coast considered here U_m is $-Q_{wx}/h$).

Thus (4.41) becomes

$$\frac{\partial}{\partial x}\left(\left(D_C h + \int_{-h_0}^{\bar{\zeta}} \nu_{tx} dz\right)\frac{\partial V_0}{\partial x}\right) - \frac{\tau_{b2}(V_0)}{\rho} - \frac{\partial}{\partial x}(F_2 V_0) = \frac{1}{\rho}\frac{\partial S_{xy}}{\partial x} + \frac{\partial F_1}{\partial x} \tag{4.52}$$

The solution of this equation gives the variation of the bottom velocity $V_0(x)$ in the cross shore direction and it represents—as mentioned earlier—the last condition required to determine the integration constants in the solutions given above for the total three dimensional current profiles $(U(x,z), V(x,z))$.

Preliminary Discussion of Results

It is worth already at this point to notice that the additional terms in (4.52) originating from the current-current interactions (D_C, F_1 & F_2) of course depends on the driving forces α_x and α_y as defined by (4.31) and (4.35). They depend only on the cross- shore current-velocity profile $U(x,z)$, however, seemingly not on the longshore velocity V itself which means that (4.52) is really a linear equation for V_0 (at least as long as a linear relationship is used for $\tau_{by}(V_0)$ but this is not a necessary condition for the validity of (4.52)).

Both by the seemingly total dependence on the cross-shore velocity profile, and in respect to the way in which the vertical eddy viscosity ν_{tz} enter the value of D_C, the results are completely parallel to the results for the longitudinal dispersion in a pipe found by Taylor (1954), and the dispersion coefficient for three dimensional continental shelf currents given by Fischer (1978). The additional effect here is the direct influence from the waves represented by the second term in D_C and by F_1 and F_2.

The results also deviate from the above mentioned earlier results, in particular those of Fischer, by the deceiving way in which D_C, F_1 and F_2 all depend also on the longshore velocity profiles. From the expressions (4.39) and (4.48)–(4.51) for those quantities, one may get the (false) impression that the dispersion effect they represent exists even for a depth uniform longshore current. That situation, however, would correspond to $V_1 = 0$ which, as (4.30) shows, would cause all dispersion effects to vanish. The clue to this paradox lies in equation (4.34) which shows that if there is a longshore radiation stress (represented by α_y) and a longshore current gradient (a $\partial V_0/\partial x$) then the first integral in (4.34) is generally non-zero and the second term will be so as well. Hence, a depth uniform longshore current is not a consistent solution to the present problem. Or, in other words, although D_C, F_1

and F_2 seem independent on the longshore current profile, that profile is intimately linked to the same mechanism that generated D_C, F_1 and F_2.

5 NUMERICAL RESULTS

The results obtained so far are fairly general as they apply to arbitrary variations over depth of the driving terms α_x and α_y as well as the eddy viscosities ν_{tx} and ν_{tz}.

To illustrate the nature of the variations which can be expected, it is instructive to consider the special case of $\nu_{tx} = \nu_{tz} = \nu_t =$ constant over depth and α_x, α_y similarly depth uniform. In this case, the expressions for U_1 and $V = V_0 + V_1$ can be written as

$$\begin{aligned} U_1 &= a_x\,\xi^2 + b_x\xi + U_b \\ V &= a_y\xi^2 + b_y\xi + V_b + A(\xi)\frac{\partial V_0}{\partial x} \end{aligned} \tag{5.1}$$

where we will neglect V_{b1} (see eq. (4.16) for justification) so that $V_b = V_0$ and where

$$a_x = \frac{1}{2}\,\frac{\alpha_x}{\nu_{tz}} \quad ; \quad b_x = \frac{\tau_{bx}}{\rho\nu_{tz}} \tag{5.2}$$

$$a_y = \frac{1}{2}\,\frac{\alpha_y}{\nu_{tz}} \quad ; \quad b_y = \frac{\tau_{by}}{\rho\nu_{tz}} \tag{5.3}$$

are functions of the local meanwater depth $h(= h_0 + \bar{\zeta})$ through the way in which α_x, α_y, ν_{tz} are specified. For τ_{bx} we have from (4.8)

$$\tau_{bx} = \frac{1}{\pi}\rho\, f\, u_{wb}\, U_b \tag{5.4}$$

which means that

$$b_x = \frac{f u_{wb}}{\pi\nu_{tz}} U_b = b\, U_b \tag{5.5}$$

where b (independent of U_b) is defined by (4.12).

Invoking (4.13) for the depth integral of U, substituting (5.5) for τ_{bx} and solving for U_b we get

$$U_b = U_m \cdot \frac{1 + \frac{1}{3}\frac{a_x h^2}{U_m}}{1 + \frac{bh}{2}} \tag{5.6}$$

which means $U(x,z)$ is completely determined.

Thus in this simplified case, the results for D_C, F_1 and F_2 can be expressed in terms of the parameters a_x, a_y which essentially represent the driving forces from the cross- and longshore radiation stresses, the parameter b, linking ν_{tz}, the bottom friction parameter and the wave motion together, and ν_{tz} the (vertical) eddy viscosity. U_m the depth averaged cross shore mean velocity is also a parameter.

Typical values of U_m are $-(0.03 - 0.1)\sqrt{gh}$ (see e.g., Svendsen et al., 1987). From the same source, we assess α_x mainly on the basis of $\partial\bar{\zeta}/\partial x$ which in the surf zone typically is 10% of the undisturbed bottom slope, h_{0x}. Together with an estimated ν_{tz} of $0.01h\sqrt{gh}$ (4.31) then yields for $h_{0x} = 1/30$ that $a'_x \sim 0.15$ where $a'_x = a_x h^2/\sqrt{gh}$.

A realistic value of $f \sim 2 \cdot 10^{-2}$ (see e.g., Jonsson & Karlsen, 1976) gives $b' \sim 0.1$ where $b' = bh$.

These values are used as guidelines for the choice of parameter values for the numerical results shown below.

Fig. 4 shows the variation of $D'_C = D_C\,(\overline{\nu_{tz}}/U_m^2 h^2)$ for $b' = b'_x = 0$ and $a'_x = 0$, 0.1 and 0.2 versus U_m. Although there clearly would be a dispersion effect even in the (unrealistic) case of a depth uniform undertow ($a_x = 0$), it is also clear that the usual depth variation of the undertow current ($a_x \neq 0$) greatly enhances the dispersion effect.

It may be mentioned that although D'_C grows for $U_m \to 0$, $D_C = (U_m^2 h^2/\nu_{tz})\,D'_C$ does

tend to zero in that limit as one would expect.

As indicated by (4.46), D_C is composed of two contributions, I_A and I_D. Of those, I_D is analogous to the dispersion coefficient found by Fischer (1978) for three dimensional currents on the continental shelf; whereas I_A, representing interaction between the waves and the currents, is new. The numerical computations show that I_A is the dominating term.

Fig. 5 shows the corresponding undertow profiles for the typical case of $U'_m = -0.06$.

In Figs. 4 and 5, b has been chosen to be zero. As has been found many times in the past (see particularly Svendsen & Hansen, 1988), the cross-shore bottom shear stress is quite small and exercises a very weak influence on the undertow velocity profile. Accordingly, it is found that the curves for D_C for $b' = 0$, 0.1 and 0.2 can hardly be distinguished from one another. Consequently, the results in Fig. 4 for $b = 0$ (i.e., no mean cross-shore bottom shear stress) are representative for all reasonable values of b.

On the basis of Fig. 4, it is possible to give a crude estimate of the magnitude of D_C relative to ν_{tx}. For the case $\nu_{tz} = \nu_{tx} = \overline{\nu_{tz}}$, we get from (4.46)

$$\frac{D_C}{\nu_{tx}} = \frac{U_m^2 h^2}{\overline{\nu_{tz}^2}} (\alpha_e I_a - I_D)$$

Here we have $U_m h = -Q_{wx}$ and a typical value of Q_{wx} is $0.06h\sqrt{gh}$, which means Q_{wx} is approximately $5\,\overline{\nu_{tz}}$. At the same time, Fig. 4 shows that $\alpha_e I_a - I_D \sim 0.5$ which suggests that $D_C/\nu_{tx} = 0(10)$. In the example in Section 6, the D_C value turns out to be approximately $17\,\nu_{tx}$.

The expression for the dispersion coefficient D_C also includes the turbulent eddy viscosity ν_{tz}, both directly and through U_1/U_m where ν_{tz} occurs both in a_x and b_x. The computations in Fig. 6 are for α_x in the range found for the experimental results analyzed by Svendsen et al. (1987), and with $b = 0$ (and hence $b_x = 0$). We see that in the range of ν_{tz} values

around 0.01 $h\sqrt{gh}$ found in experiments, there is a substantial variation of D'_C which grows with decreasing ν_{tz}. This essentially is equivalent to the growing curvature on the undertow velocity profile with growing a_x shown in Fig. 5. Since decreasing ν_{tz} represents decreasing turbulence from breaking, this will usually also be associated with a decline in the slope $\partial\bar{\zeta}/\partial x$ on the mean water level and hence, in Fig. 6, a reduction in α_x. No firm relation between the two parameters is available but it means that for real wave situations, the variation of D'_C with ν_{tz} will be much more moderate than indicated by the α_x = const curves in Fig. 6.

The significance of the assumption that the longshore current profile determined below trough level can be continued into the region between trough and crest of the waves can be illustrated by varying the parameter α_e defined by (4.40). Fig. 7 shows a realistic range of α_e values. $\alpha_e = 1.0$ essentially corresponds to a linear extrapolation of the velocity profile above wave trough. $\alpha_e = 1.1$ thus retains a positive curvature ($\partial^2 V/\partial z^2 > 0$) whereas $\alpha_e = 0.9$ represents a situation with $\partial^2 V/\partial z^2 < 0$ above trough level. This figure, in which $a_x = 0.1$, may be compared with Fig. 4 (which corresponds to $\alpha_e = 1.0$). Clearly, there is an effect from this assumption but the nature of the results for D_C does not seem seriously affected.

Finally, results are shown in Figs. 8 and 9 for the two integrals I_{ca} and I_{cb} in the additional terms in the equation (4.52) for V_0, again versus U'_m.

It may also be mentioned that in the numerical evaluation of all the integrals, such as I_A, I_D, I_{ca} and I_{cb}, where the time averaging includes the entire integral, the results contain terms of the form $\overline{d^n}$ where $d = h + \eta$. Hence, strictly speaking, these results can only be evaluated correctly if the wave surface profile $\eta(t)$ is known. It turns out, however, that for most wave forms and for the wave height to water depth ratios of 0.5–0.7 common in the nearshore region, it is a reasonable approximation to set $d^n \simeq h^n$. As an example, for a sine

wave with $\gamma = H/h = 0.6$, we get $\overline{d^2} = 1.05h^2$, $\overline{d^3} = 1.14h^3$ and $\overline{d^4} = 1.27h^4$. Furthermore, the magnitude of the terms in the results decrease with increasing power of d.

6 CURRENT VELOCITIES ON A STRAIGHT COAST

In the present section, equation (4.52) is solved for the cross-shore variation $V_b(x)$ of the longshore velocity at the bottom on a plane beach. The solution also provides results for the vertical profiles of U and V in the regions inside and outside the surf zone.

The solutions are developed under the simplifying assumption that sine wave theory is applicable for the calculation of the radiation stresses, and the assumption of a constant wave height to water depth ratio, γ, inside the surf zone. Outside the breaker point, Green's law of $H \propto h^{-\frac{1}{4}}$ is applied.

Since these assumptions are known to give rather inaccurate representations of the actual conditions on a beach, in particular for the situation inside the surf zone, they imply that the results given are generic. The purpose is to illustrate the nature of three dimensional current patterns and the effect of the mechanisms considered.

The distinction between wave conditions before and after breaking implies that at the breaking point ($h = h_b$) we have discontinuities in several of the driving parameters. Thus, $\partial S_{xy}/\partial x$ jumps from zero outside the surf zone to a finite value at the breaking point and throughout the surf zone we get

$$\frac{\partial S_{xy}}{\partial x} = \frac{5}{16}\gamma^2\rho(gh)^{\frac{3}{2}}\left(\frac{\sin\alpha_w}{c}\right)_\infty h_x \tag{6.1}$$

Also, α_x and α_y, and hence a_x and a_y are discontinuous at $h = h_b$ which influences the vertical velocity profiles and thereby the longshore current distribution $V_b(x)$.

Thus, the solution of (4.52) from the shoreline to deep water is a matched combination of

the solutions inside and outside the breaker point. The boundary and matching conditions for the solution of (4.52) is as follows:

$$V_b = 0 \quad \text{at} \quad \begin{cases} h = 0 \\ h/h_b \to \infty \end{cases} \tag{6.2}$$

$$V_b(x_b+) = V_b(x_b-) \tag{6.3}$$

$$\frac{\partial V}{\partial x}\Big)_{x_{b+}} = \frac{\partial V}{\partial x}\Big)_{x_{b-}} \tag{6.4}$$

Here x_b represents the breaker line position, and the last condition is equivalent of continuity in τ_{xy}, the horizontal shear stresses in the longshore direction along vertical shore parallel surfaces.

To simplify the discussions, a'_x is assumed constant in the surf zone. This is in accordance with the assumption of γ = const which yields $\partial\bar{\zeta}/\partial x$ constant (Bowen et al., 1968). As indicated in section 5, a characteristic value corresponds to $a'_x \sim 0.15$. Invoking (4.2) for nondimensionalizing (U, U_b) and (4.43) for ξ, we can then write (5.1) as

$$U' = a'_x\, \xi^{*2} + b'_x \xi^* + U'_b \tag{6.5}$$

which is evaluated inside the surf zone with the above mentioned $a'_x = 0.15$.

The longshore driving force represented by α_y is in the computations assumed to correspond to an angle of incidence for the waves of 11.4° at the breaker point which yields $v_w \sim 0.2\, u_w$ or $\overline{u_w v_w} \sim 0.2\, \overline{u_w^2}$. For linear theory with $u_w \sim c\eta/h$ and $\gamma = 0.7$ this gives

$$\frac{\partial}{\partial x}\overline{u_w w_w} \sim 0.2 \cdot g h_x \gamma^2 \overline{\eta^2}/H^2 \sim 0.012 g h_x$$

which is approximately $\alpha_x/10$.

Outside the surf zone however, the picture is significantly different, mainly because of the lack of energy dissipation, which implies that $\partial\bar{\zeta}/\partial x$ is quite small. Using, again, linear theory we get

$$\frac{\partial\bar{\zeta}}{\partial x} = \frac{3}{32}\left(\frac{H}{h}\right)^2 h_x - \frac{\tau_b}{\rho g h} \tag{6.6}$$

$$\frac{\partial\overline{u_w^2}}{\partial x} = -\frac{3}{32} g \left(\frac{H}{h}\right)^2 h_x \tag{6.7}$$

Invoking the arguments given in section 4 for $\partial\overline{u_w w_w}/\partial z$, this then yields

$$\alpha_x = g\frac{\partial\bar{\zeta}}{\partial x} + \frac{1}{2}\frac{\partial\overline{u_w^2}}{\partial x} \tag{6.8}$$

or, by virtue of (6.6) and (6.7)

$$\alpha_x = -\frac{\tau_b}{\rho h} \tag{6.9}$$

which is much smaller than α_x inside the surf zone.

Thus, below trough level the setup gradient and the wave radiation stresses balance each other except for the small contribution from the bottom friction.

At the same time, the steady streaming in the bottom boundary layer, which was shown by Svendsen et al. (1987) to have a negligible effect on the undertow inside the surf zone, modifies the cross-shore profiles by significantly reducing the (seaward oriented) bottom velocity U_b. In the computations of this effect, we have essentially followed Svendsen & Hansen (1988).

In the surf zone, the eddy viscosity ν_t is chosen as $0.01h\sqrt{gh}$. Outside the surf zone, however, ν_{tx} and ν_{tz} are expected to decrease as we move seaward. Very little information is available, even of the level of turbulent kinetic energy k in (1.5). Fig. 10 from Nadaoka & Kondoh (1982) shows the only known measurements of k outside the breaker point. The

results indicate that although k deceases, the level of turbulence outside the breaker point is not negligible and does not seem to vanish completely even several times the surf zone width seaward of the breaker point. Based on these observations, we have used the following expression for $\nu_t = \nu_{tx} = \nu_{tz}$:

$$\nu_t = \begin{cases} 0.01h\sqrt{gh^2} & \text{inside surf zone} \\ [0.8(h/h_b)^4 + 0.2]\nu_{tb} & \text{outside surf zone} \end{cases} \tag{6.10}$$

where $\nu_{tb} = 0.01h_b\sqrt{gh_b}$

As reference and comparison for the computations are used computations that largely correspond to Longuet-Higgins' analytical solution (L-H, 1970) which is based on similar assumptions as the computations reported here regarding the use of linear wave theory even in the surf zone, and the expression (4.8) for the bottom friction. The mass flux Q_{wx} for breaking waves (which is not part of the L-H solution) has again been taken as $Q_{wx} = 0.12(H^2/h)\sqrt{gh}$ (which yields $U_m = -0.06\sqrt{gh}$ inside the surf zone for $\gamma = 0.7$).

Our numerical reference computations as well as the solution of (4.52) and associated equations also deviate from the analytical L-H solution by using Greens law for the wave height variation outside the breaker point (against $\gamma = H/h =$ constant used in the analytical (L-H) solution). Since $\partial S_{xy}/\partial x = 0$ outside the breaker point, the major effect of this is the equivalent change of τ_b through the change of u_{wb} in (4.8).

Fig. 11 shows the results of four different computations of $V_b(x)$ on a 1/30 slope beach. One (marked a) corresponds to the L-H solution with $\nu_t = 0.01h\sqrt{gh}$ everywhere. This means ν_t increasing seaward as $h^{\frac{3}{2}}$ even outside the break point. The solution marked b shows the effect of using the eddy viscosity given by (6.10). In both these cases, the dispersion effects represented by D_C and the other interaction terms in (4.52) have been neglected. We see that the effect of changing the already small eddy viscosity ν_t outside the surf zone is very modest indeed.

The curve marked c represents the results from solving (4.52) including D_C and the F_1 and F_2 terms in combination with the solutions for the vertical profiles for the currents U & V and ν_t given by (6.10).

Finally, curve d represents a computation similar to b (i.e., with no dispersion effects) but with ν_t increased to a level that gives the same maximum longshore current velocity as found in computation c. This turns out to require $\nu_t = 0.17h\sqrt{gh}$, or 17 times the eddy viscosity used in case c. In terms of Longuet-Higgins' P, the curves have $P = 0.005$ (a, b & c) and $P = 0.085$ (curve d). This latter value of P is in accordance with what has, generally, been found gives the best agreement with measurements for $V(x)$, with the approximations made about use of linear theory and linearized bottom friction.

Thus, it is found that for the example considered in these computations, the effect of the dispersion has provided a longshore current variation equivalent to what measurements usually indicate while keeping the eddy viscosity at values compatible with the estimates we can justify from turbulence measurements.

Simultaneously, with the computation of V_b the solutions for $U(x,z)$ and $V(x,z)$ are obtained as indicated earlier. These profiles are shown in Figs. 12 and 13 for the parameter values and assumptions corresponding to case c in Fig. 11.

In the absence of steady streaming, with the many simplifications introduced, there is only one undertow velocity profile inside the surf zone. The inclusion of steady streaming introduces less than 10% variability of the undertow cross-shore location. The profiles outside the breaker point decrease with increasing depth which reflects the general decrease seaward of wave heights and forcing.

The complicated variations in the neighborhood of the break point must necessarily be rather schematically represented by the simple discontinuities in wave conditions assumed at

the point. In agreement with what was mentioned earlier, the shape of the undertow profiles outside the surf zone are remarkably different from those inside, the bottom velocities being quite small, and the velocity increasing upwards from bottom. This almost triangular shape is in fact in agreement with the available measurements from that region (see e.g., Nadaoka & Kondoh (1982), Fig. 14.

The longshore current profiles also show an interesting shift near the breaker point. Outside that point, these currents are entirely driven by the dispersion mechanisms described above and the (much weaker) turbulent mixing. The realism of these profiles is therefore a very sensitive indicator of the—at least qualitative—accuracy of the description of the dispersive mechanism.

For all positions, we find that $V(x,z)$ only vary slightly over the depth. Hence, the cross-shore distribution of V_b in Fig. 11 is really characteristic for the entire variation of the longshore current velocity field. Fig. 13 also shows, however, that from the shoreline and till a depth of about 0.8 h_b, the longshore current velocities increase slightly from the seabed towards the surface. From $h = 0.8h_b$ and seaward, this tendency is reversed and the maximum value of $V(z)$ now appears at the bottom.

Recalling that a depth uniform V yields no dispersion effects whatsoever, this shift in the sign of $\partial V/\partial z$ indicates a similar shift in the sign of the dispersion effect, represented in the equation essentially by the change of sign of $\partial^2 V/\partial x^2$ around the same depth.

The significance of this change in the shape of longshore current profiles as we go seaward is further enhanced by examination of the (only) experimental information available about the vertical profiles of the longshore currents (see Visser, 1984). These measurements are shown in Fig. 15. It is remarkable that all Visser's profiles show exactly the same pattern as predicted by the present method: $\partial V/\partial z > 0$ for $h \leq h_b$ and $\partial V/\partial z < 0$ seaward of that

point. Given the important connection between this feature and the dispersion mechanism, this qualitative agreement between measurements and theory seems very encouraging.

Finally, it is mentioned that a direct quantitative comparison with experimentally measured longshore current velocities has deliberately been omitted. To make sense such comparisons would require a much more accurate evaluation of radiation stresses and other wave properties. The accuracy of the rather crude model for the time averaged bottom shear stress would also have to be more closely examined.

7 CONCLUSIONS

It has been shown that the three-dimensional structure of the cross- and longshore currents, generated on a beach by the breaking waves, plays a crucial role in the horizontal distribution of these currents. A perturbation solution of the full set of equations on a long straight beach leads to analytical representations of the three-dimensional effect which is dispersive in nature. It corresponds to a generalization of the longitudinal dispersion effect found by Taylor (1954) for flow in a pipe and by Fischer (1978) for ocean currents on the continental shelf. In addition to these mechanisms, the dispersion in the nearshore region includes an interaction with the wave mass flux which is the largest contribution. For typical nearshore conditions, the effect is found to be 10–20 times stronger than the turbulent lateral mixing that can be justified on the basis of our knowledge of the turbulence inside and outside the surf zone.

Accordingly, it is found that the shape of the cross-shore variations of the longshore currents typically found in the literature can be predicted with a turbulent lateral mixing that is one to two orders of magnitude smaller than what is normally assumed and which falls within the bounds of what can be justified from turbulence measurements.

Simultaneous with the longshore current profiles, results are also obtained for the vertical structure of cross- and longshore currents. It is shown that these results show characteristics differences in and outside the breaker point and these differences are found to be in qualitative agreement with experimental results.

ACKNOWLEDGEMENTS

The authors gratefully acknowledge important references to the literature from K. Nadaoka and N. Kobayashi. This work is a result of research sponsored by NOAA Office of Sea Grant, Department of Commerce, under Grant No. NA86AA-D-SG040 (Project No. R/OE-6). The U.S. Government is authorized to produce and distribute reprints for government purposes notwithstanding any copyright notation that may appear herein.

REFERENCES

Battjes, J. A., 1975. Modelling of turbulence in the surf-zone. *Proceedings of a Symposium on Modelling Techniques*, ASCE, San Francisco, pp. 1050–61.

Bowen, A. J., 1969. The generation of longshore currents on a plane beach. *Journal of Marine Research*, 27, pp. 206–215.

Bowen, A. J. and D. L. Inman, 1974. Nearshore mixing due to waves and wave induced currents. *Rapp. P.-v. Reun. Cons. Int.*, 167, pp. 6–12.

Bowen, A. J., D. L. Inman and V. P. Simmons, 1968, Wave 'set-down' and set-up. *Journal of Geophysical Research*, 73, pp. 2569–2577.

Brevik, I., 1980. Flume experiment on waves and currents. II. Smooth bed. *Coastal Engineering*, 4, 2, 89–110.

Brevik, I. and B. Aas, 1980. Flume experiment on waves and currents. I. Rippled bed. *Coastal Engineering*, 3, 149– 177.

Christoffersen, J. B. and I. G. Jonsson, 1985. Bed friction and dissipation in a combined current and wave motion. *Ocean Engineering*, 12, 5, 387–423.

Dally, W. R. and R. G. Dean, 1984. Suspended sediment transport and beach profile evolution. *Journal Waterway, Port, Coastal and Ocean Engineering*, ASCE, 110, WW1, 15–33.

Deigaard, R. and J. Fredsoe, 1989. Shear stress distribution in dissipative water waves. *Coastal Engineering*, 13, 4, 357–378.

Fischer, H. B., 1978. On the tensor form of the bulk dispersion coefficient in a bounded skewed shear flow. *Journal of Geophysical Research*, 83, pp. 2373–2375.

Grant, W. D. and O. S. Madsen, 1979. Combined wave and current interaction with a rough bottom. *Journal of Geophysical Research*, 84 , 1797– 1808.

Hansen, J. B. and I. A. Svendsen, 1987. The cross-shore motion over a barred beach profile. *Proc. Conf. Eng. Devel. Countries*, Beijing.

Harris, T. F. W., J. M. Jordan, W. R. McMurray, C. J. Verwey and F. P. Anderson, 1963. Mixing in the surf zone. *International Journal of Air and Water Pollution*, 7, pp. 649–667.

Inman, D. L., R. J. Tait and C. E. Nordstrom, 1971. Mixing in the surf zone. *Journal of Geophysical Research*, 76, pp. 3493–3514.

Jensen, B. L., B. M. Sumer and J. Fredsoe, 1989. Turbulent oscillatory boundary layers at high Reynolds numbers. *Journal of Fluid Mechanics*, 206, 265–297.

Jonsson, I. G., 1966. Wave boundary layers and friction factors. *Proceedings of the 10th Coastal Engineering Conference*, pp. 127–148.

Jonsson, I. G. and N. A. Carlsen, 1976. Experimental and theoretical investigations in an oscillatory turbulent boundary layer. *J. Hydro. Research*, 14, 1, 45–60.

Kemp, P. H. and R. R. Simons, 1982. The interaction between waves and a turbulent current; waves with the current. *Journal of Fluid Mechanics*, 116, 227.

Kemp, P. H. and R. R. Simons, 1983. The interaction of waves and a turbulent current: Waves propagating against the current. *Journal of Fluid Mechanics*, 130, 73–89.

Longuet-Higgins, M. S., 1970. Longshore currents generated by obliquely incident sea waves. Parts 1 and 2. *Journal of Geophysical Research*, 75, pp. 6778–6789 and pp. 6790–6801.

Longuet-Higgins, M. S. and R. W. Stewart, 1960. Changes in the form of short gravity waves on long waves and tidal currents. *Journal of Fluid Mechanics*, 13, pp. 481–504.

Longuet-Higgins, M. S. and R. W. Stewart, 1964, Radiation stress in water waves, a physical discussion with application. *Deep Sea Research*, 11, pp. 529–563.

Liu, P. L.-F. and R. A. Dalrymple, 1978. Bottom frictional stresses and longshore currents due to waves with large angles of incidence. *Journal of Marine Research*, 36, pp. 357–375.

Mei, C. C. 1983. *The Applied Dynamics of Ocean Surface Waves.* John Wiley and Sons, New York, 740 pp.

Nadaoka, K., and T. Kondoh, 1982, Laboratory measurements of velocity field structure in the surf zone by LDV. *Coastal Engineering in Japan*, 25, pp. 125–145.

Okayasu, A., T. Shibayama and K. Horikawa, 1988. Vertical variation of undertow in the surf-zone. *Proceedings of the 21st Coastal Engineering Conference*, pp. 478–491.

Okayasu, A., T. Shibayama and N. Mimura, 1986. Velocity field under plunging waves. *Proceedings of the 20th Coastal Engineering Conference*, pp. 660–674.

Phillips, O. M., 1977. *The Dynamics of the Upper Ocean.* Cambridge University Press, 336 pp.

Stive, M. J. F. and H. G. Wind, 1986. Cross-shore mean flow in the surf-zone. *Coastal Engineering*, 10, pp. 325–340.

Svendsen, I. A., 1984. Mass flux and undertow in a surf-zone. *Coastal Engineering*, 8, pp. 347–365.

Svendsen, I. A. 1987. Analysis of surf zone turbulence. *Journal of Geophysical Research*, 92, pp. 5115–24.

Svendsen, I. A. and J. B. Hansen, 1988. Cross-shore currents in surf-zone modelling. *Coastal Engineering*, 12, pp. 23–42.

Svendsen, I. A. and R. S. Lorenz, 1989. Velocities in combined undertow and longshore currents. *Coastal Engineering*, 13, pp. 55–79.

Svendsen, I. A. and Putrevu, U. 1990. Nearshore circulation with 3-D profiles. *Proceedings of the 22nd Coastal Engineering Conference*, pp. 241–254.

Svendsen, I. A., H. A. Schaffer and J. B. Hansen, 1987. The interaction between the undertow and boundary layer flow on a beach. *Journal of Geophysical Research*, 92, pp. 11,845–856.

Taylor, G. I., 1954. The dispersion of matter in a turbulent flow through a pipe. *Proceedings of the Royal Society of London.* Series A, 219, pp. 446–468.

Thornton, E. B., 1970. Variation of longshore current across the surf zone. *Proceedings of the 12th Coastal Engineering Conference*, pp. 291–308.

Trowbridge, J. H. and O. S. Madsen, 1984. Turbulent wave boundary layers, parts 1 & 2. *Journal of Geophysical Research*, 89, pp. 7989–8007.

Visser, P. J., 1984. A mathematical model of uniform longshore currents and comparison with laboratory data. Communications on Hydraulics. *Report 84-2*, Department of Civil Engineering, Delft University of Technology, 151 pp.

List of Figures

Fig. 11 Computed cross-shore variations of longshore bottom velocities V_b. $\gamma = 0.7$, $f = 0.02$, $Q_w = 0.12\frac{H^2}{h}\sqrt{gh}$.

a) V_b from (4.52), without dispersion, $\nu_t = 0.01h\sqrt{gh}$ everywhere.

b) As a), ν_t given by (6.10).

c) V_b from (4.52) with dispersion. ν_t given by (6.10).

d) V_b from (4.52) without dispersion, $\nu_t = 17$ times the value given by (6.10).

Fig. 12 Cross-shore (undertow) current profiles for different values of h/h_b. Parameters and assumptions as in Fig.11, case c.

Fig. 13 Longshore current profiles for different values of h/h_b. Parameters and assumptions as in Fig. 11, case c. Note the change in $\partial V/\partial z$ around $h = 0.8h_b$.

Fig. 14 Measured undertow profiles (from Nadaoka & Kondoh 1982). Note the triangular shape of the undertow profiles outside the surf zone.

Fig.15 Measured longshore current profiles (from Visser 1984, experiment No. 2). The first three locations are inside the surf zone, the fourth location is at the point of breaking and the last four locations are outside the surf zone. Note the change in $\partial V/\partial z$ around the break point.

Figure 1

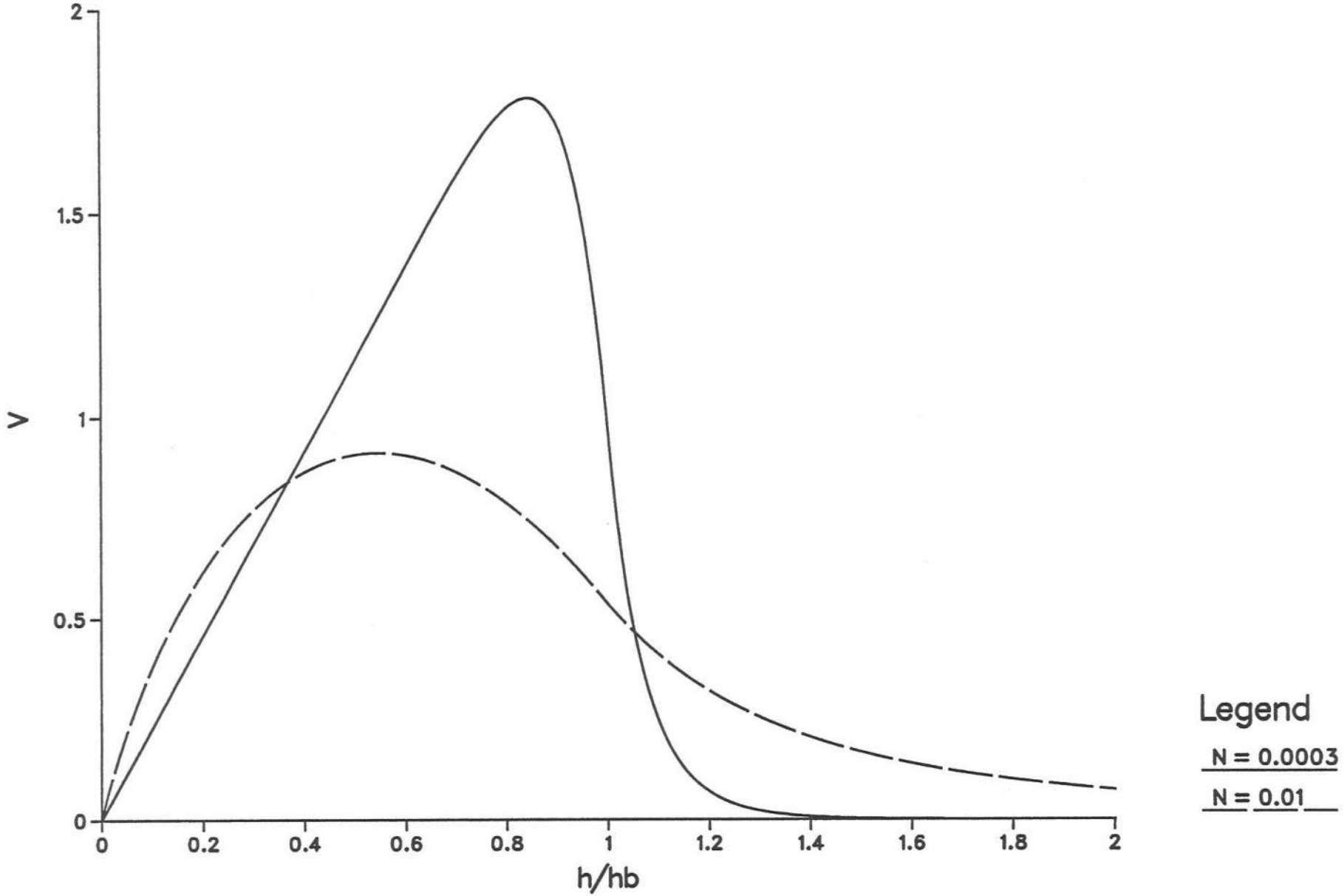

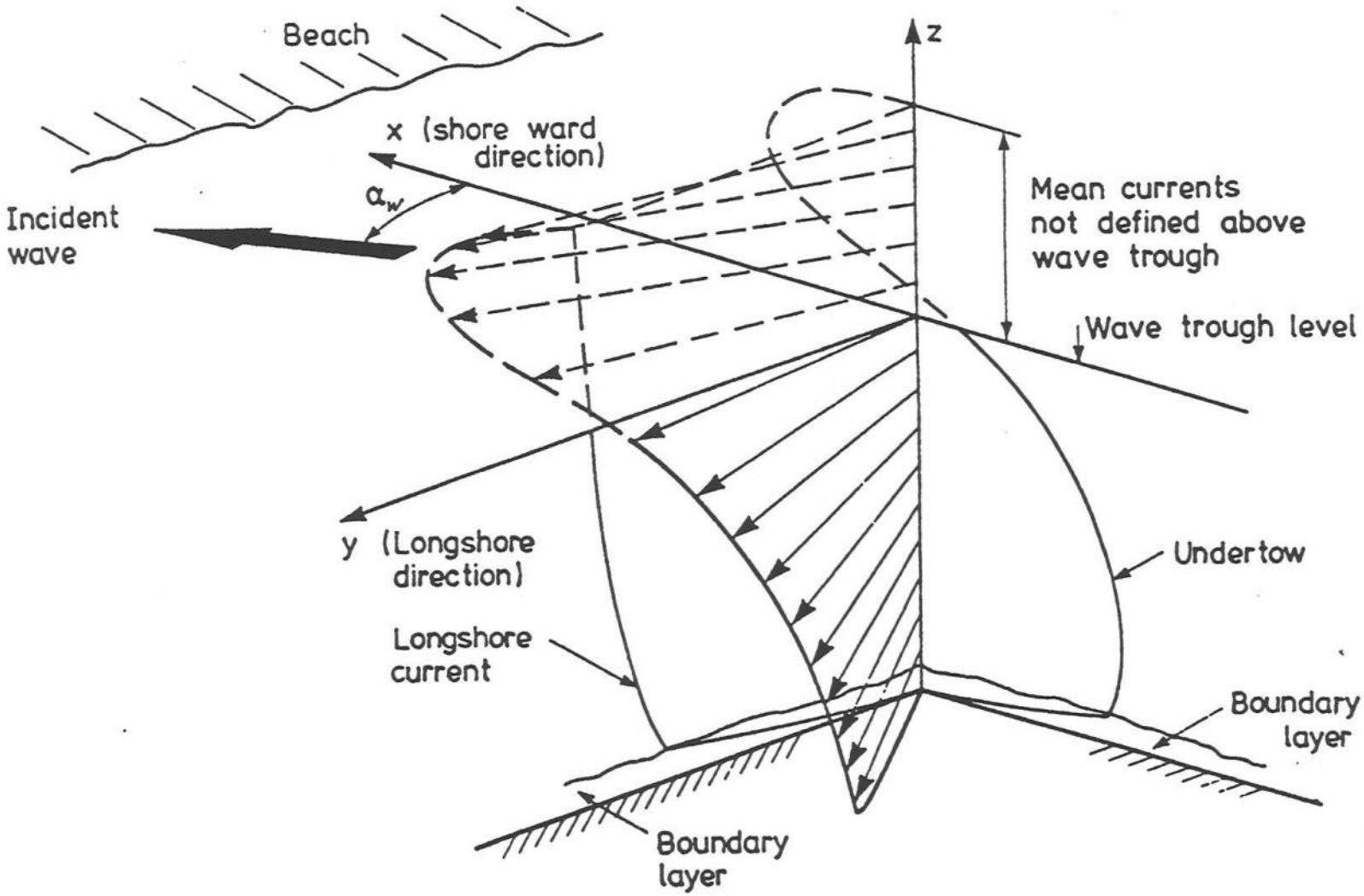
Beach
x (shore ward direction)
α_w
Incident wave
z
Mean currents not defined above wave trough
Wave trough level
y (Longshore direction)
Undertow
Longshore current
Boundary layer
Boundary layer

Figure 2.

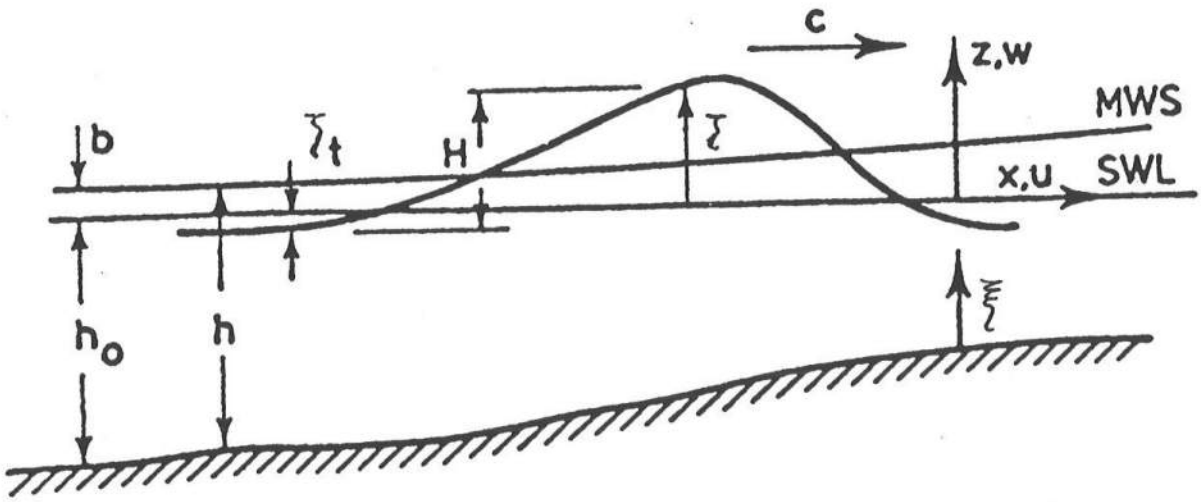

Figure 3.

Figure 4

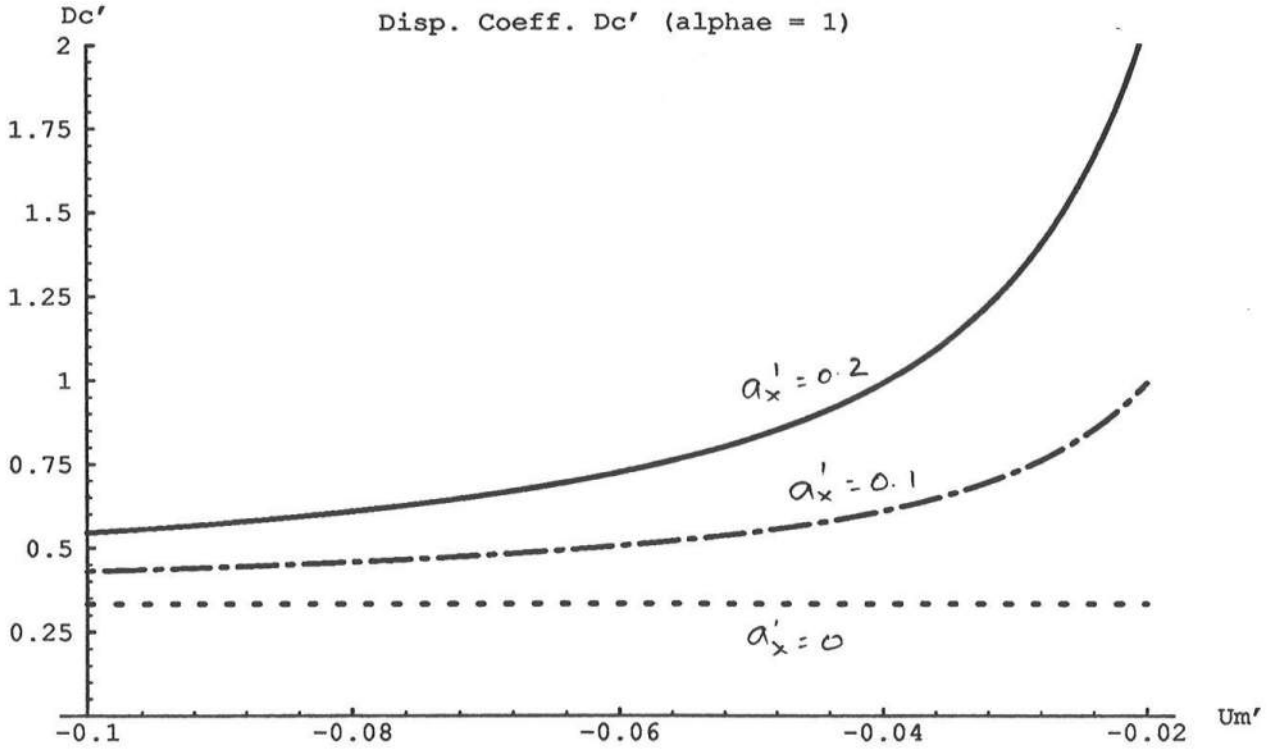
Dc'
Disp. Coeff. Dc' (alphae = 1)
2
1.75
1.5
1.25
1
0.75
0.5
0.25
$a_x' = 0.2$
$a_x' = 0.1$
$a_x' = 0$
-0.1
-0.08
-0.06
-0.04
-0.02
Um'

Figure 5

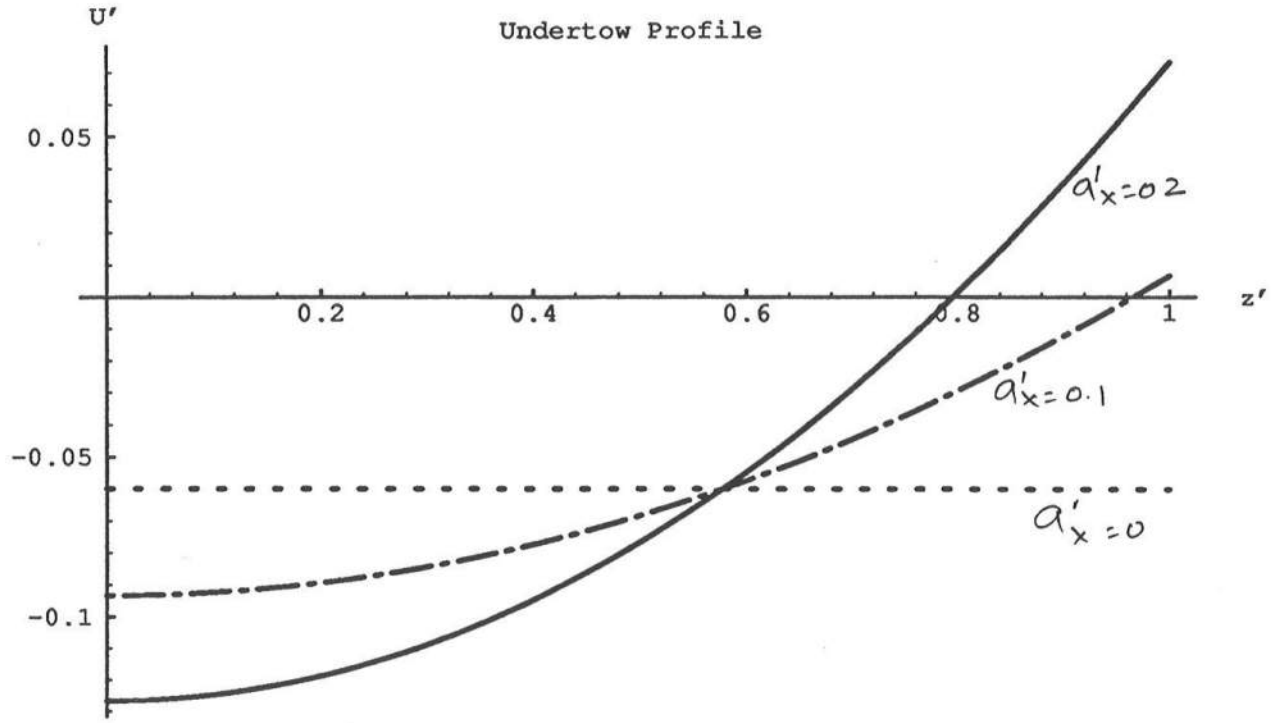

Figure 6

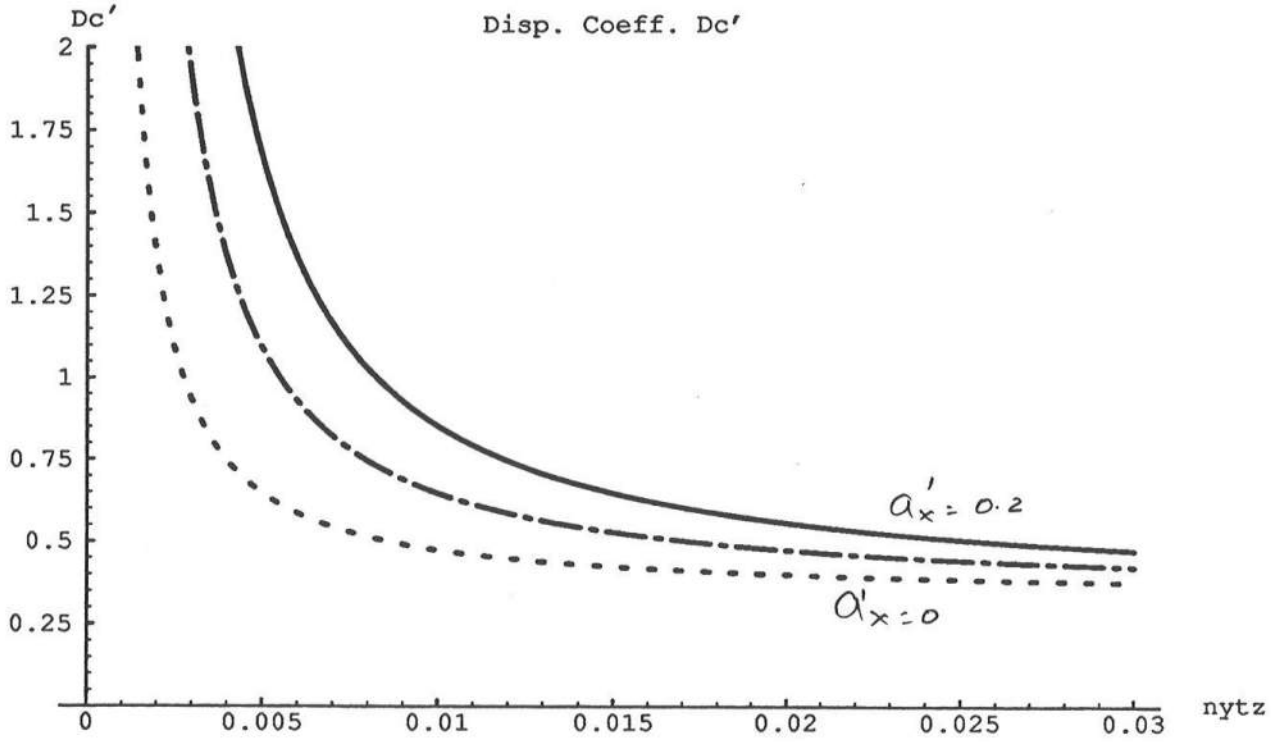
Dc'
Disp. Coeff. Dc'
2
1.75
1.5
1.25
1
0.75
0.5
0.25
0
0.005
0.01
0.015
0.02
0.025
0.03
nytz
a'x = 0.2
a'x = 0

Figure 7

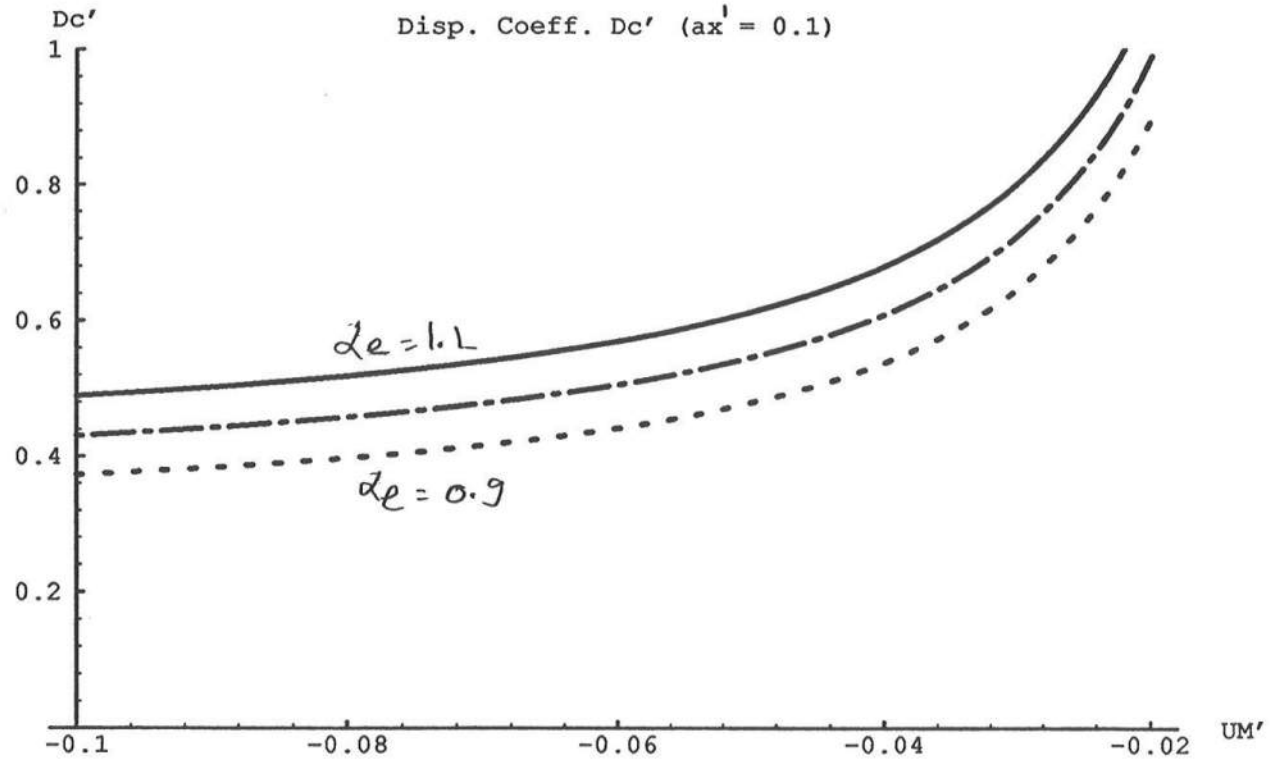
Dc'
Disp. Coeff. Dc' (ax' = 0.1)
1
0.8
0.6
0.4
0.2
$\alpha_e = 1.1$
$\alpha_e = 0.9$
-0.1
-0.08
-0.06
-0.04
-0.02
UM'

Figure 8

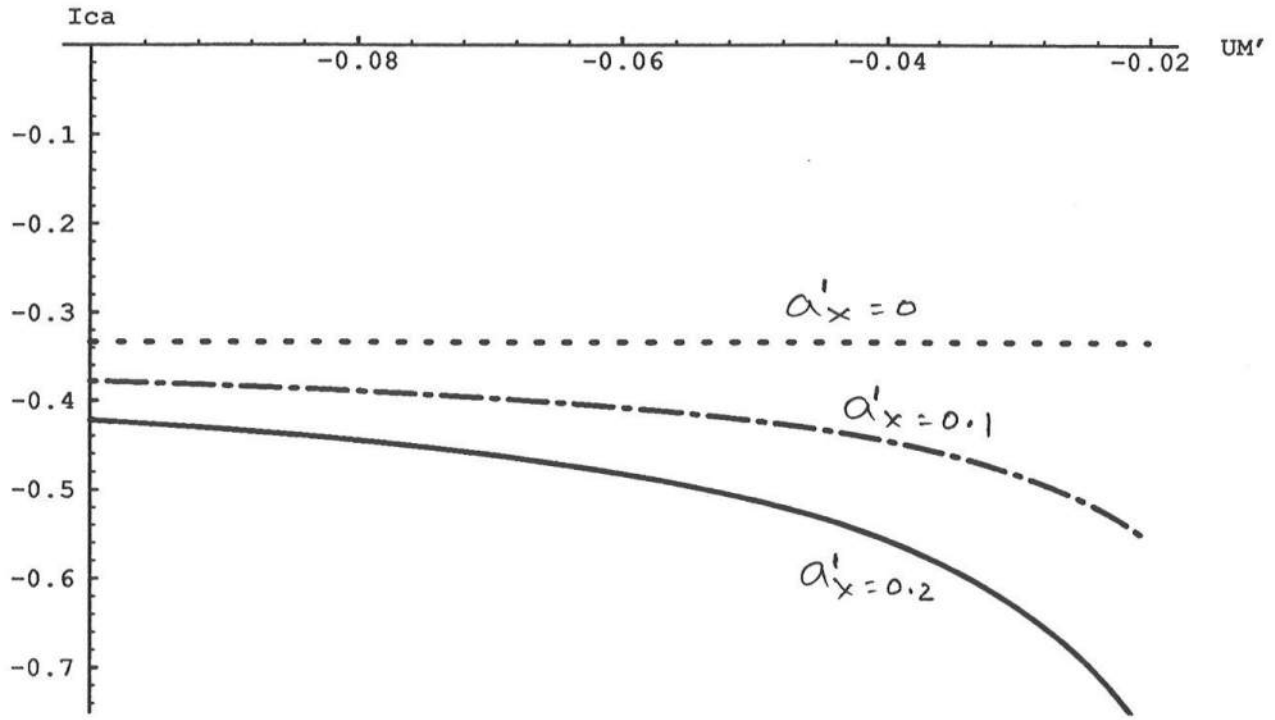

Figure 9

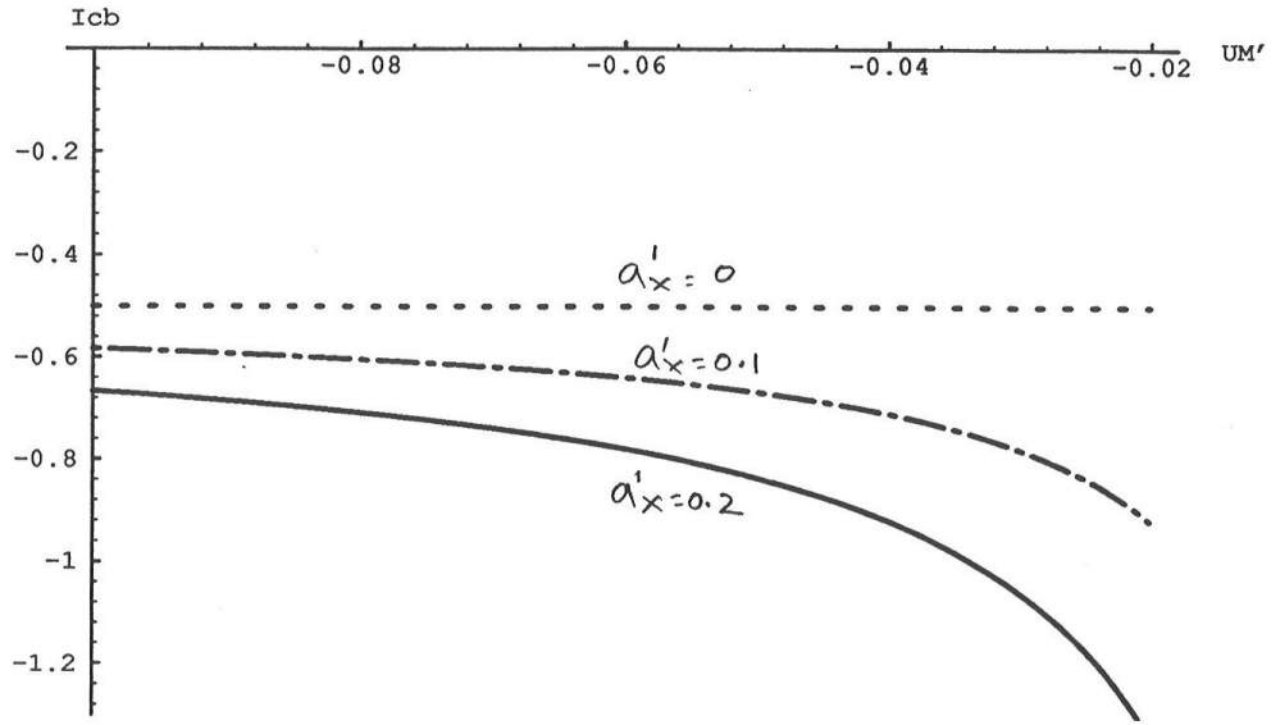

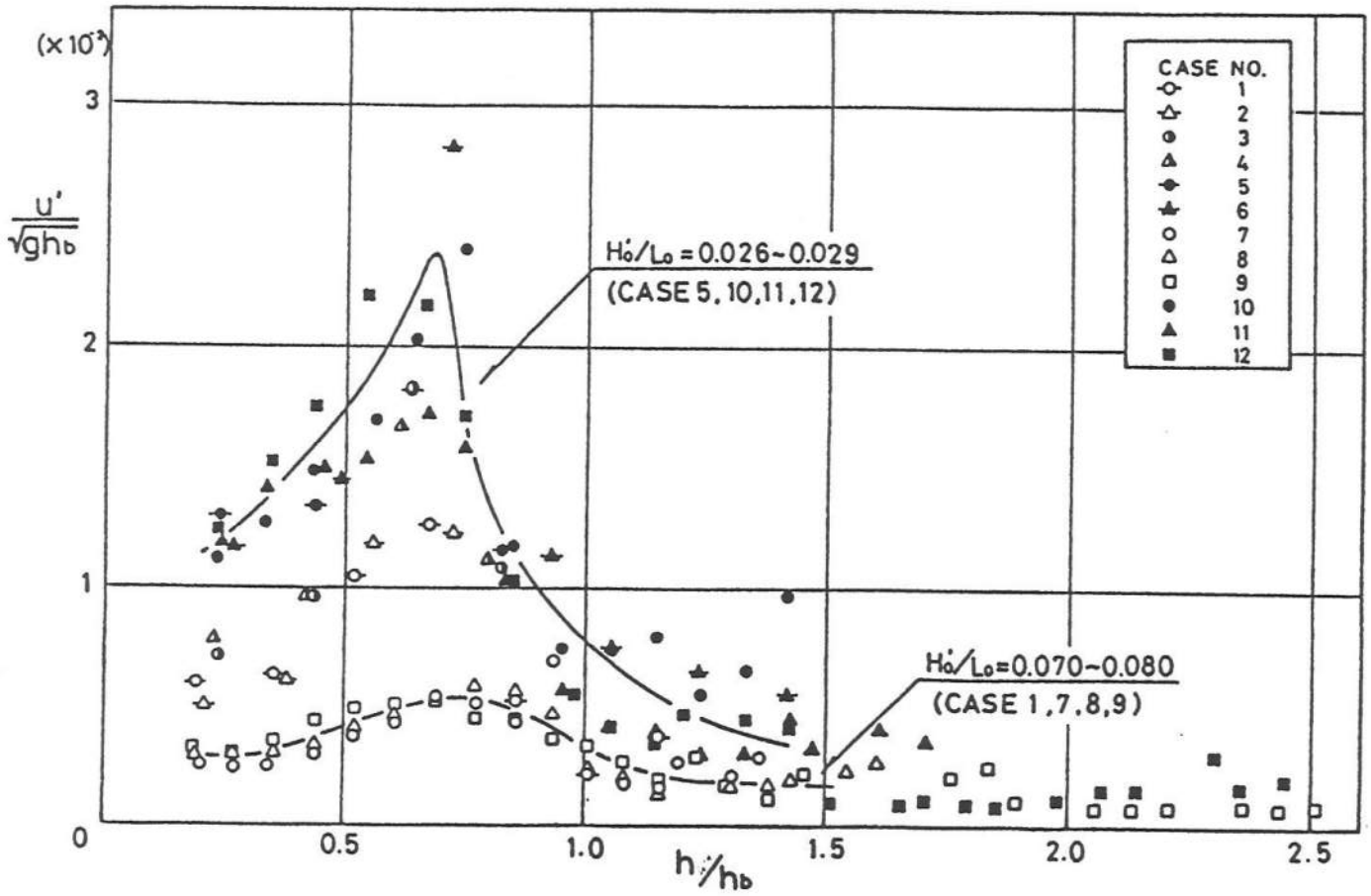
(×10⁻²)
3
2
1
0
u'/√ghb
H0/L0 = 0.026~0.029
(CASE 5, 10, 11, 12)
H0/L0=0.070~0.080
(CASE 1, 7, 8, 9)
CASE NO.
1
2
3
4
5
6
7
8
9
10
11
12
0.5
1.0
1.5
2.0
2.5
h'/hb

Fig 10

Figure 11

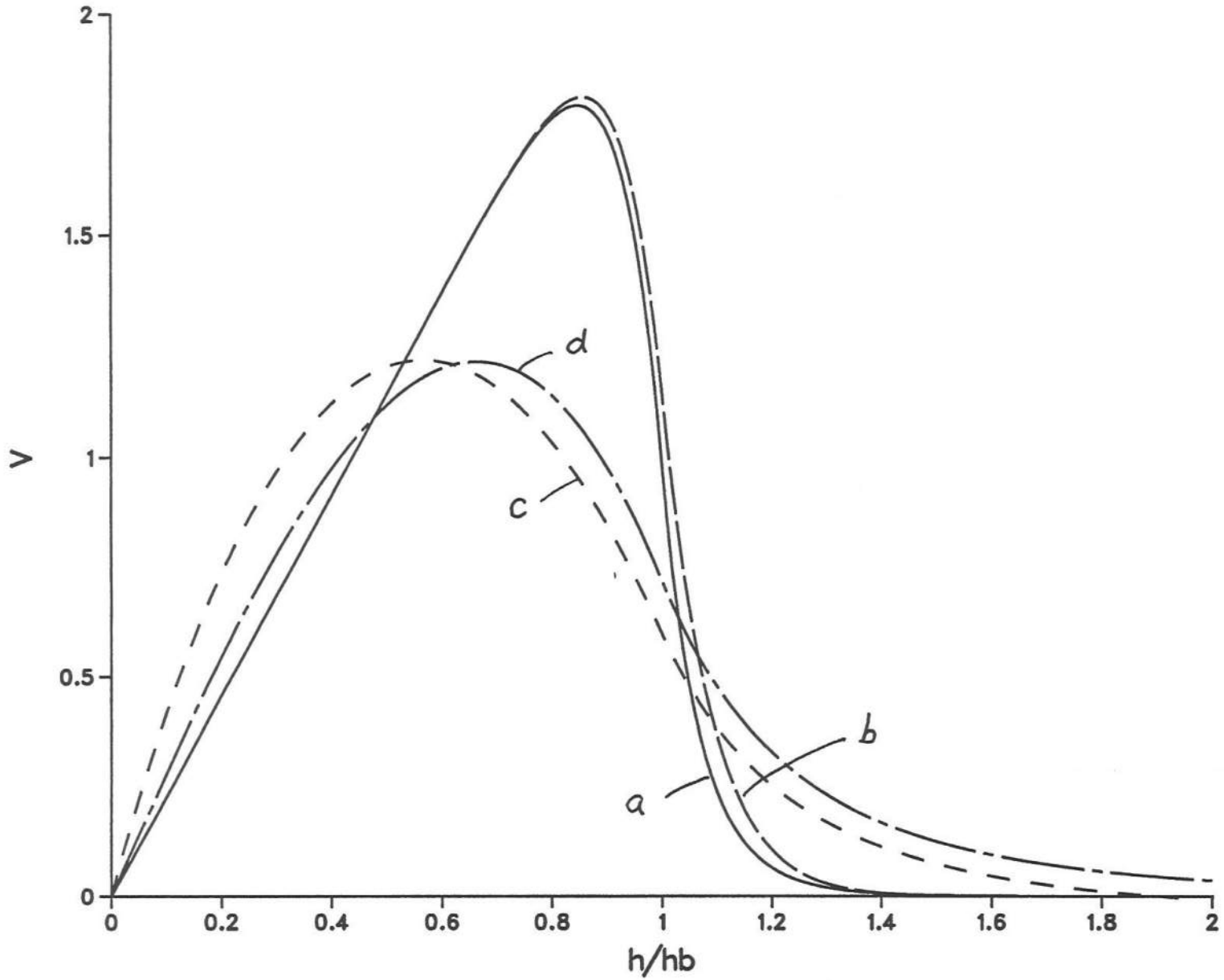

Figure 12

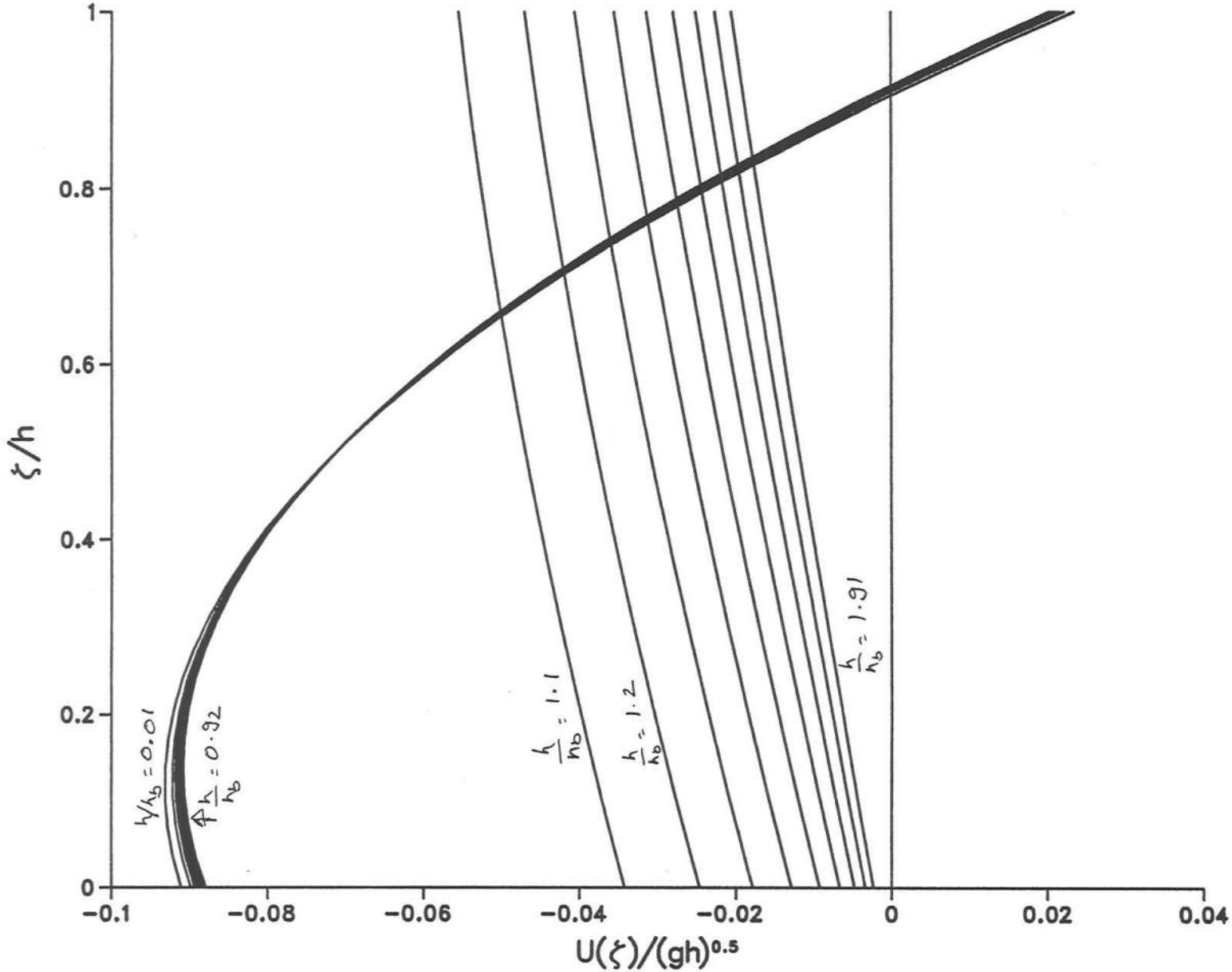
1
0.8
0.6
0.4
0.2
0
ζ/h
−0.1
−0.08
−0.06
−0.04
−0.02
0
0.02
0.04
U(ζ)/(gh)^0.5
h/h_b = 0.01
h/h_b = 0.92
h/h_b = 1.1
h/h_b = 1.2
h/h_b = 1.91

Figure 13

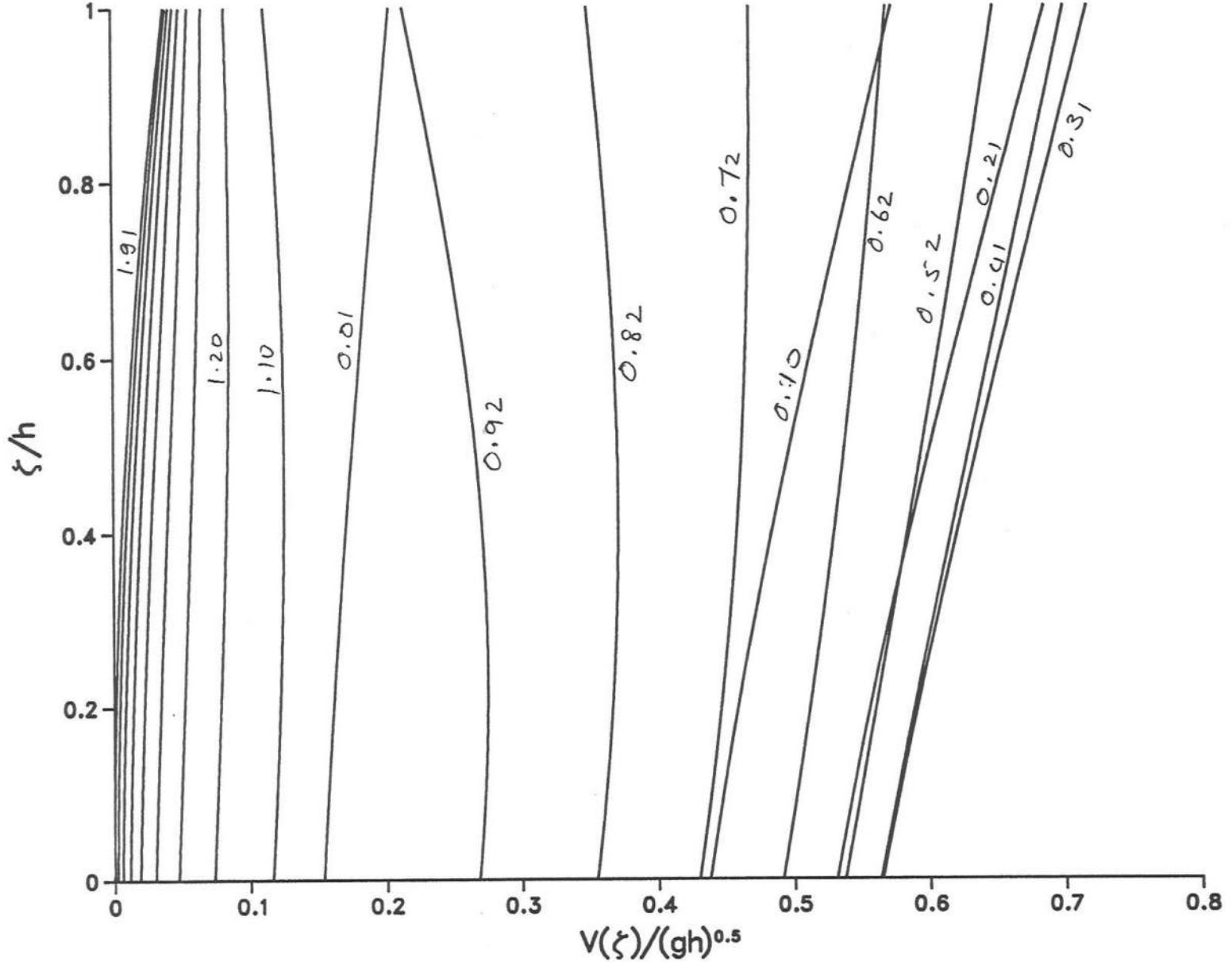
1
0.8
0.6
0.4
0.2
0
ζ/h
0
0.1
0.2
0.3
0.4
0.5
0.6
0.7
0.8
V(ζ)/(gh)^0.5
1.91
1.20
1.10
0.01
0.92
0.82
0.72
0.10
0.62
0.52
0.41
0.21
0.31

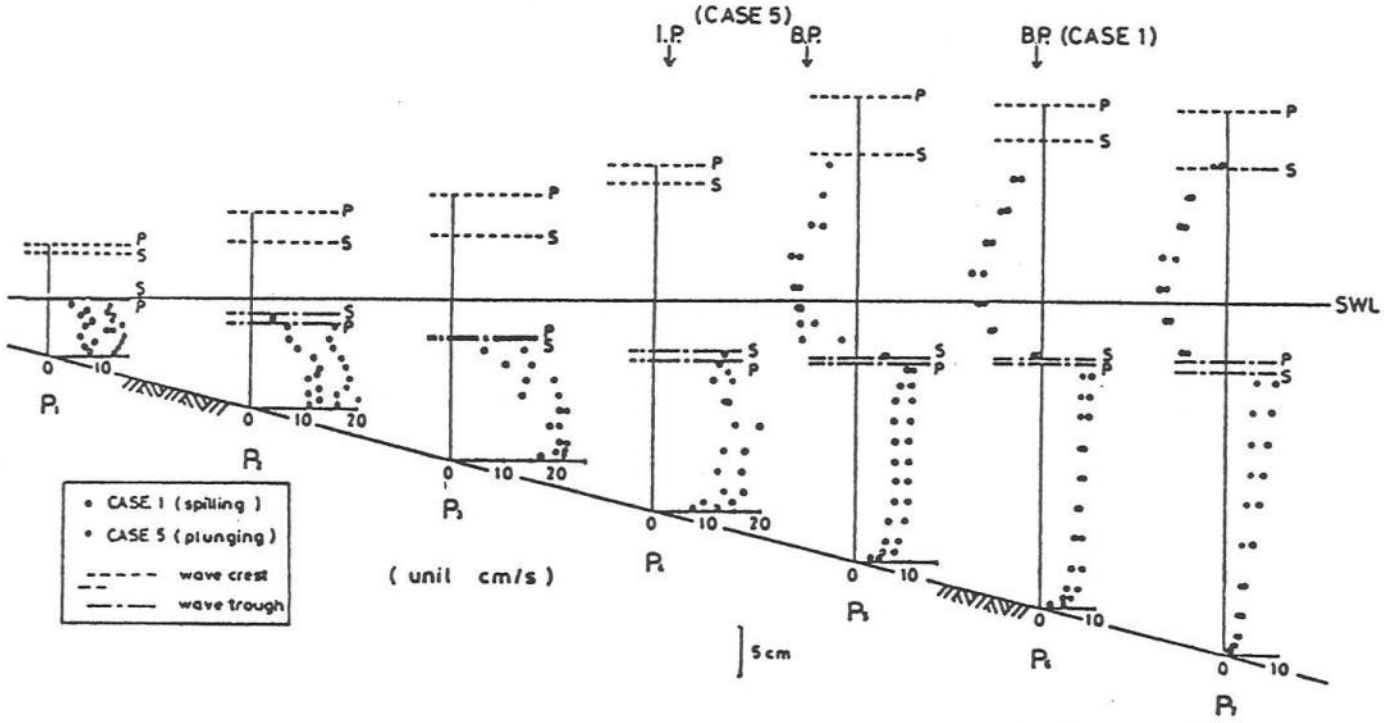
(CASE 5)
I.P.
B.P.
B.P. (CASE 1)
SWL
P
S
0
10
20
P1
P2
P3
P4
P5
P6
P7
• CASE 1 (spilling)
• CASE 5 (plunging)
wave crest
wave trough
(unit cm/s)
5cm

FIGURE 14

FIGURE 15

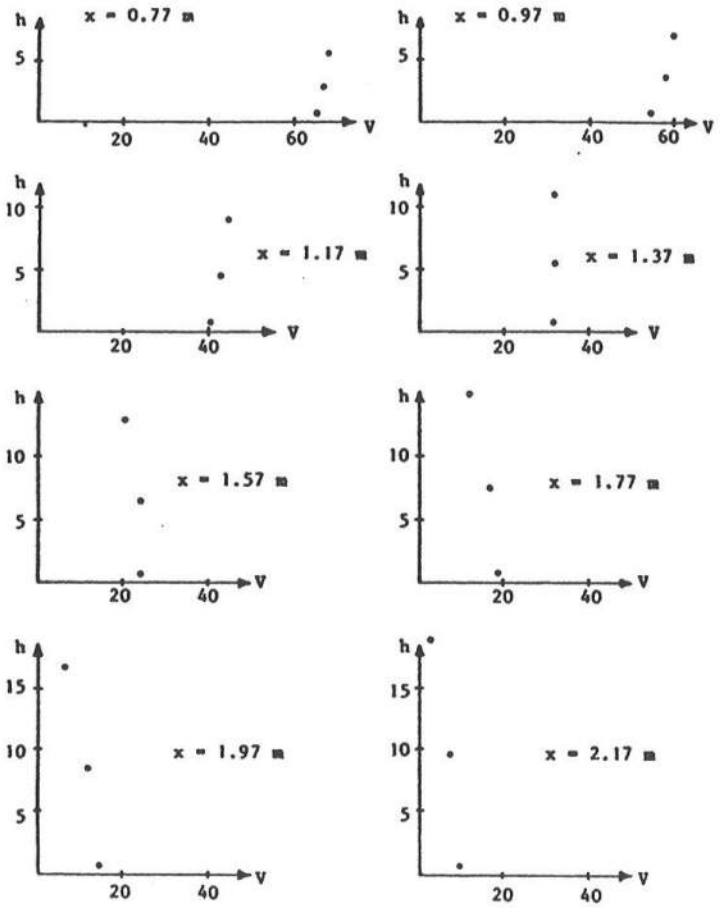
x = 0.77 m
x = 0.97 m
x = 1.17 m
x = 1.37 m
x = 1.57 m
x = 1.77 m
x = 1.97 m
x = 2.17 m
h
V
5
10
15
20
40
60